

See discussions, stats, and author profiles for this publication at: <https://www.researchgate.net/publication/51085368>

# Petroleum Analysis

ARTICLE *in* ANALYTICAL CHEMISTRY · JUNE 2011

Impact Factor: 5.64 · DOI: 10.1021/ac201080e · Source: PubMed

---

CITATIONS

61

---

READS

57

## 2 AUTHORS, INCLUDING:



Amy M. Mckenna

Florida State University

54 PUBLICATIONS 980 CITATIONS

SEE PROFILE

# Petroleum Analysis

Ryan P. Rodgers\*,†,‡ and Amy M. McKenna†

\*National High Magnetic Field Laboratory, Florida State University, 1800 East Paul Dirac Drive, Tallahassee, Florida 32310, United States

†Department of Chemistry and Biochemistry, Florida State University, 95 Chieftan Way, Tallahassee, FL 32306–4390, United States

## CONTENTS

Mass Spectrometry for Petroleum Analysis	4666	Asphaltene Fractionation	4677
Advances in Ionization	4666	Solubility Parameter	4677
Atmospheric Pressure Ionization	4666	Nuclear Magnetic Resonance	4677
Laser Induced Desorption	4666	NMR for Asphaltene Characterization	4678
Atmospheric Pressure Photoionization	4666	Aggregation	4678
Electrospray Ionization	4666	Structure	4678
Laser Desorption/Ionization	4667	Fluorescence	4679
Probe MS and FI/FD	4667	Fluorescence Spectroscopy: Reservoir	4679
Inductively Coupled Plasma (ICP)	4667	Characterization	4679
Mass Spectrometry Applications	4668	Optical Spectroscopy	4679
Whole Crude Oil and Hydrocarbons	4668	Fluorescence Correlation Spectroscopy	4679
Nitrogen	4668	Time-Resolved Fluorescence	4679
Sulfur	4669	Centrifuge and Ultrafiltration	4679
Metals	4669	High-Q Ultrasonic Spectroscopy	4680
Naphthenic Acids, Naphthenates, and Neutral	4670	X-ray Photoelectron Spectroscopy	4680
Nitrogen	4670	Small Angle X-ray Scattering	4680
Asphaltenes	4671	Small Angle Neutron Scattering	4680
Asphaltene Molecular Weight	4671	Advances in Asphaltene Characterization	4681
Asphaltene Composition/Structure	4672	Direct-Current (dc) Electrical Conductivity	4681
Geochemistry	4672	Liquid Crystal Asphaltenes	4681
Separations	4674	Petroleomics	4682
Recent Advances in Gas Chromatography	4674	Author Information	4682
Paraffins and Waxes	4674	Biographies	4682
Nitrogen	4674	Acknowledgment	4682
Pyrolysis GC	4674	Nomenclature	4683
Simulated Distillation	4674	References	4683
Composition-Explicit or Advanced Distillation Curve	4675		
Multidimensional Gas Chromatography	4675		
Targeted Multidimensional Gas Chromatography	4675		
Comprehensive Two-Dimensional Gas Chromatography (2D-GC or GC × GC)	4675		
Industrial Applications of GC × GC	4675		
Nitrogen	4675		
Sulfur	4675		
Supercritical Fluid Chromatography and Extraction	4676		
Size-Exclusion Chromatography	4676		
Capillary Electrophoresis (CE)	4676		
High-Performance Liquid Chromatography	4676		
Adsorption Chromatography	4677		

After a nearly decade absence, we present a review of noteworthy contributions in petroleum analysis over the past 3 years, intentionally limited to ~250 references. The global shift to heavier petroleum slates, the exploration/production of unconventional petroleum reserves, and a growth in deep- and ultradeep water production platforms is reflected in the number of publications herein that address heavy crude oil, acids, metals, reservoir architecture, and production deposit characterization. Advances in mass spectrometry, comprehensive gas chromatography, and hybrid analytical platforms have led to an

**Special Issue:** Fundamental and Applied Reviews in Analytical Chemistry

**Published:** April 29, 2011



explosion in the accessible detailed (molecular-level) compositional information. Cross fertilization of compositional data provided by multiple analytical techniques clarify many issues that have been hotly debated for decades. First and foremost, the molecular weight of petroleum is now known, and claims of abundant, "high molecular weight" species (>2000 Da) are compromised by aggregation. The compositional complexity of petroleum is immense, with as many as 250 peaks identified over a single nominal mass but evolves in composition (as boiling point increases) in a predictable manner. Concern in regards to the metal content and speciation of organometallic components of heavy conventional and unconventional crude oils will continue its current trend and grow rapidly in the coming years. Petroleomics was born in an attempt to expand the pioneering work in the correlation/prediction of petroleum behavior/reactivity from detailed compositional data. High field FT-ICR mass spectrometers are now common in petroleum R&D centers where they were absent less than a decade ago. Molecular level information has become essential but has not quite found a home. The ability to generate information has exceeded our ability to consume and use it to shape decisions. Thus, the next push in the field will be to develop models (predictive tools) to capture the wealth of information now available.

## ■ MASS SPECTROMETRY FOR PETROLEUM ANALYSIS

**Advances in Ionization.** *Atmospheric Pressure Ionization.* Advances in petroleum analysis have always been intimately tied to advances in mass spectrometry ionization sources and instrumentation. Until the advent of big pharma, the reverse was also true; advances in instrumentation and ionization methods were largely driven by the ever present need for more advanced petroleum analyses. Oddly enough, the recent spotlight on energy research has brought the relationship full circle, as many new ionization methods are developed to address the compositional complexity of petroleum derived materials. Electrospray ionization (ESI) of petroleum materials was first demonstrated by low-resolution MS by Fenn et al.<sup>1</sup> in the late 1990s and soon after was coupled to high-resolution Fourier transform ion cyclotron resonance mass spectrometry (FT-ICR MS),<sup>2,3</sup> that made it possible to address the compositional complexity of the acidic and basic species in crude oil at the molecular level. Combined with the pioneering work of Quann and Jaffe,<sup>4</sup> Fenn's demonstration of the utility of electrospray ionization for petroleum analysis launched the field of Petroleomics. Simply, the previous ionization difficulties with polar fractions of crude oil now facilitated their direct detection in petroleum without prior fractionation. Eberlin et al. exploited ESI-type ionization mechanisms (protonation and deprotonation) in easy ambient sonic-spray ionization (EASI) to demonstrate the detailed compositional analysis of acidic and basic species in petroleum<sup>5</sup> and fuels.<sup>6</sup> The method, based on supersonic spray, requires no voltage change for operation in either the  $-/+$  mode, sample preparation is minimal, and the compositional information afforded is near identical to that of ESI. Other ambient techniques such as desorption electrospray ionization (DESI) and direct analysis in real time (DART) emerged concurrently. Wu et al. introduced reactive DESI for the analysis of saturated hydrocarbons in petroleum distillates.<sup>7</sup> In a noteworthy departure from other ionization methods, reactive DESI targets the abundant, nonpolar alkanes through a deliberately produced electric discharge and a derivatization reagent. The subsequent oxidation products were

detected by ion trap or orbitrap mass spectrometry and compared to conventional field ionization (FI) time-of-flight results. Rummel et al. coupled a custom-built DART source to a FT-ICR mass spectrometer to evaluate applications in polycyclic aromatic hydrocarbon (PAH) and crude oil analysis.<sup>8</sup> As highlighted by the high field FT-ICR MS data, DART successfully produced both radical and protonated molecular ions for the PAH standards and crude oil, but as with DESI, was limited to low boiling components.

*Laser Induced Desorption.* Pioneered by Kenttämäa<sup>9</sup> as a vacuum technique, laser induced acoustic desorption (LIAD) has recently been developed as an atmospheric pressure desorption method. Nyadong et al. modified an atmospheric pressure photoionization (APPI) source to allow for LIAD desorption of petroleum samples with subsequent chemical ionization (CI) and detection by FT-ICR MS.<sup>10</sup> Inclusion of a dopant gas allows ionization to be tuned for the desired ion type and analyte chemistry without fragmentation as revealed by the analysis of petroleum and biomarker-type standards. Analysis of a bitumen distillation cut revealed the direct characterization of abundant heteroatom-containing species at a mass resolving power commensurate with conventional ionization methods (400 000 at  $m/z = 400$ ). Goa et al. followed with a similar LIAD-CI technique performed on a low-resolution ion trap that evaluated methanol/water, benzene, and carbon disulfide reagents.<sup>11</sup> Carbon disulfide, which produced radical and protonated molecular ions, performed well for all standards and minimized unwanted fragmentation. The LIAD-CI analysis (without reagent) of a high boiling distillate cut suggests efficient desorption/ionization of high boiling species (supported by LIAD-electron ionization (EI) results obtained in vacuo), but the most abundant species in the mass spectrum were attributed to fragment ions.

*Atmospheric Pressure Photoionization.* Conventional atmospheric pressure ion sources (ESI and APPI) have been recently updated with microfabricated devices. Atmospheric pressure photo-ionization, initially introduced by Purcell et al. for petroleum characterization,<sup>12</sup> was demonstrated with a microchip APPI source ( $\mu$ APPI) coupled to FT-ICR MS.<sup>13</sup> Haapala et al. displayed similar performance (signal stability, molecular weight, compositional coverage, and reproducibility) equal to a conventional APPI source but at flow rates 25-fold lower than previously possible. The disproportional loss in sensitivity ( $\sim$ 2-fold) relative to the reduced flow rate (25-fold), combined with the elimination of sample carryover and thus, elimination of repeated source maintenance, make the technique attractive for 1 chip/1 analysis sample introduction.

*Electrospray Ionization.* ESI emerged as an automated technique for the analysis of large sample sets with the demonstration of 20 h (50 sample) continuous +ESI analysis of light, medium, and heavy crude oil samples.<sup>14</sup> Kim et al. successfully analyzed 10 samples (5 replicates each) with a NanoMate (Advion BioSciences Inc.) coupled to a FT-ICR mass spectrometer. The ion source was modified to permit the use of glass 96-well plates with an aluminum foil compression fitting to prevent sample evaporation over the extended analysis times. Compositional coverage was indistinguishable from conventional ESI analysis and allowed spectral averaging of the replicates to increase the dynamic range. Sensitivity in APCI was addressed by Kim et al. by modification of conventional two-component solvent blends to a single component (toluene) solvent system.<sup>15</sup> Results of the toluene APCI experiments were similar to those obtained by dopant assisted APPI; therefore, charge-transfer reactions were implicated in the formation of molecular ions.

**Laser Desorption/Ionization.** A multimode chip-ESI and atmospheric pressure laser ionization (cESILI) ion source was introduced by Schmitt-Kopplin et al. to expand the compositional coverage beyond that of conventional ESI.<sup>16</sup> Both + and - ion modes were demonstrated with FT-ICR MS detection and revealed increased compositional complexity relative to the cESI only results. Two-step laser mass spectrometry ( $L^2MS$ )<sup>17</sup> was applied to the analysis of asphaltenes in an effort to avoid aggregation of desorbed species (high molecular weight artifacts) previously suggested by Hortal et al.<sup>18</sup> and systematically studied by Tanaka<sup>19</sup> and later by Apicella.<sup>20</sup> The  $L^2MS$  experiment employs two different wavelength laser pulses that are spatially and temporally separated. A CO<sub>2</sub> laser (0.1 eV at 10.6 μm) pulse desorbs the sample that is subsequently ionized by a pulse of 4.7 eV photons (266 nm). The molecular weight distribution is insensitive to delay time, concentration (2 orders of magnitude), and desorption/ionization energies, all which greatly affect the molecular weight distributions measured by LDI. The author's followed with a more detailed study of the technique that analyzed asphaltenes isolated from different crudes and a comparison to coal asphaltenes.<sup>21</sup> Hurtado et al. published a useful summary of one- and two-step laser desorption ionization methods that employed a variety of laser wavelengths. Briefly, one step UV-LDI easily induces aggregation whereas one-step IR-LDI and two-step UV/UV- $L^2MS$  and IR/UV- $L^2MS$  largely suppress aggregate formation and thus yield a more accurate, reproducible molecular weight determination for high-boiling petroleum species.<sup>22</sup> Sabbah et al. studied the  $L^2MS$  fragmentation behavior of nine "asphaltenic" standards to understand the structural origins of fragmentation.<sup>23</sup> Comparison of fragmentation results from "island" and "archipelago" type structural motifs to that of an asphaltene reveal that the asphaltene fragmentation behavior is most similar to "island" type standards. Thus, the authors suggest that "island" type structures are dominant in petroleum asphaltenes.

Guo et al. investigated a novel combination of IR desorption with tunable synchrotron vacuum ultraviolet photoionization mass spectrometry (LD/VUV PIMS) for the analysis of petroleum atmospheric residue. IR desorption with near-threshold single-photon ionization allows for saturated alkane molecular weight determination analysis that varies slightly over increased photon energy (9.0–10.8 eV).<sup>24</sup> Volk et al. employed online femtosecond laser ablation with gas chromatography/mass spectrometry (GC/MS) for the analysis of petroleum from single rock/mineral inclusions for the first time.<sup>25</sup> Laser pulses (800 nm, 50 fs width, and 11 MHz repetition rate) were used to ablate material and open the inclusion. The petroleum was subsequently flushed with 100 °C He gas, cryo-focused on a Ni coil and desorbed at 320 °C for subsequent GC/MS analysis. Detailed compositional analysis of the trapped petroleum is provided for carbon numbers less than 20. The higher molecular weight material is presumed to remain in the extraction chamber due to the relatively low extraction gas temperature (100 °C). Siljeström demonstrated similar microsampling of petroleum by secondary ion mass spectrometry (SIMS) and comparison to conventional GC/MS analysis for the detection of biomarkers.<sup>26</sup> The method is proposed to access detailed compositional information from petroleum inclusions. Analysis of biomarker standards and aliphatic/nonaliphatic fractions of crude oil deposited on clean silicon wafers reveal characteristic molecular and fragment biomarker ions. Burgess et al. analyzed the monomeric components of petroleum pitch by matrix assisted

laser desorption ionization (MALDI) time-of-flight mass spectrometry and its associated dense gas extraction, gel-permeation chromatography (GPC) and high-performance liquid chromatography (HPLC) fractions to determine the main structural components by post source decay (PSD) time-of-flight (TOF).<sup>27</sup> The structural assignments were further confirmed by comparative analysis of commercially available standards.

**Probe MS and FI/FD.** Flego and co-workers demonstrated the analysis of asphaltenes by direct insertion probe-mass spectrometry and attribute differences in the molecular weight distributions of two asphaltene samples as evidence for predominately "island" type structures for one asphaltene and "archipelago" for the second.<sup>28</sup> Smith et al. demonstrated the automated FD FT-ICR MS analysis of crude oil samples with a liquid injection field desorption ionization (LIFDI) probe.<sup>29</sup> Repeated sample introduction was performed by a HTS PAL LEAP autosampler and allowed 100 coadded experiments that increased the dynamic range, resolving power, mass accuracy and molecular weight range compared to optimized single application experiments. Qian et al. presented an evaluation of FD ionization for the determination of molecular weight distributions for hydrocarbon polymers, heavy petroleum distillation cuts, and chemical/solubility cuts of heavy petroleum and compared the results to those obtained by ESI.<sup>30</sup> Although known to be selective toward polar species, the ESI molecular weight measurements generally agreed well with those obtained by FD, which targets a much wider range of chemical compositions. The authors note that the magnitude of the slightly lower ESI measured molecular weight increases with boiling point.

**Inductively Coupled Plasma (ICP).** Maryutina et al. reported a novel approach to the elemental analysis of petroleum by continuous introduction of analyte into a rotating coil column for preconcentration and subsequent analysis by ICP MS.<sup>31</sup> Caumette and co-workers examined the source of signal suppression in the analysis of organic matrices by ICP MS. Plasma ionization efficiency (quenching) was found to be the primary cause of sensitivity loss and alleviated the problem by a total consumption micronebulizer combined with a heated spray chamber. The improvements facilitated the direct multielement analysis of undiluted fuels that, due to the absence of dilution, led to a 3–4 fold increase in sensitivity over conventional methods.<sup>32</sup> Ricard et al. reported similar findings in the direct analysis of trace elements in crude oil but employed a high-repetition-rate femtosecond laser to ablate crude oil components for ICP MS detection.<sup>33</sup> The work includes an informative discussion of the issues associated with viscous sample ablation (vs conventional solid samples) and transport efficiencies of ablated material. Heilmann and co-workers presented the development of a laser ablation ICP MS method for multielement determination in crude and fuel samples desorbed from a cellulosic material with high ablation rates.<sup>34</sup> No time-dependent spike/analyte fractionation was noted for metallo-organic spikes or petroleum samples and the isotope ratios of the isotopically diluted samples remained constant over the entire ablation period. Oliveira et al. determined trace metal composition of produced formation water (PFM) by online separation/preconcentration followed by ICP MS,<sup>35</sup> an important issue as government agencies move toward monitoring produced water metal contents prior to sea disposal. V, Co, and Mn were determined by standard addition whereas Cd, Pb, Ni, Zn, Mo, Fe, and U were quantitated by isotope dilution. Efforts to determine the contribution of organometallic species in the metal content of discharge waters

suggest that there is an insignificant amount of organometallic species in the produced formation water.

**Mass Spectrometry Applications.** The applications of mass spectrometry in petroleum analysis have experienced a rebirth over the past decade. Major contributors include high-resolution and high-speed mass analyzers.<sup>36</sup> FT-ICR MS in particular has made noteworthy advances in resolution<sup>37</sup> and mass accuracy<sup>38</sup> that facilitate the analysis of complex mixtures such as petroleum.<sup>39</sup> The advent of comprehensive gas chromatography (GC × GC)<sup>40</sup> and subsequent evolution to GC × GC/TOF MS, as well as many variations highlighted in this review, have made a huge impact in the field. The versatility and compositional information provided have spawned many new and exciting opportunities in petroleum science. For this reason, unlike all other sections of this review, the mass spectrometry section is categorized by application. The authors feel that the change in organization will clarify what types of mass spectrometers are best suited to address common application areas of petroleum analysis.

**Whole Crude Oil and Hydrocarbons.** McKenna and co-workers addressed the compositional continuum of petroleum of the first two papers of a five-part series that employed ( $\pm$ )ESI and (+)APPI FT-ICR MS analysis for the detailed compositional analysis of hydrocarbon and heteroatom-containing (N, O, and S) species in a bitumen distillation series.<sup>41</sup> Comparison of the class specific compositional information revealed a steady increase in carbon number and aromaticity with increased boiling cut. More importantly, comparison of hydrocarbon, one- and two-heteroatom species within a boiling cut revealed a 2–3 carbon number decrease from that of the hydrocarbon species with the addition of each heteroatom. The decrease exactly matched the continuum model proposed by Boduszynski published nearly 25 years prior. Summation of the carbon number and aromaticity coverage of all boiling cuts revealed a compositional continuum and the abundance of species with DBE values, between that of progressive PAH growth (DBE = 4 (benzene), 7 (naphthalene), 10 (anthracene) etc.), underscored the prevalence of cycloalkane structural moieties. Extension of the FT-ICR MS detailed compositional analysis of Middle Eastern boiling fractions to the limit of distillation reveals that the continuum model accurately describes all distillable petroleum fractions.<sup>42</sup> It is shown that extension of the compositional continuum to high carbon number (up to 1 MDa) cannot account for the bulk properties of asphaltenes. Thus, either asphaltenes are not high molecular weight materials (>2000 Da) or the continuity does not apply to nondistillable petroleum species.

Interestingly, Becker et al. exposed the structural component of the petroleum continuum by ion mobility mass spectrometry (IM-MS).<sup>43</sup> An ion mobility drift cell coupled to a reflectron TOF mass spectrometer provides the analysis of LD generated petroleum ions and exposes petroleum compositional complexity through resolution of species in the IMS dimension that would otherwise be unresolved in the mass spectrum. Carbon nanopowder reveals the nature of the IMS separations based on molecular structure (linear, branched, or condensed) and charge state. Separation in the IMS occurs in milliseconds and can avoid time-consuming prefractionation steps. The analysis of a Middle Eastern light crude oil demonstrates the increase in peak capacity of the IM-MS instrument. A complementary IM-MS and separate FT-ICR MS analysis of light, medium, and heavy crude oils revealed the ability

of IM-MS to rapidly fingerprint multiple, abundant conformational classes and combined with the detailed compositional analysis of FT-ICR MS, reveals the increased structural diversity of heteroatom-containing species in heavier crude oils.<sup>44</sup> Additionally, the IM-MS data shows a shift from planar to more compact three-dimensional structures with increased mass. Thus, higher mass components result from noncovalent aggregation rather than progressive growth of planar structures.

Strausz et al. report the detailed chemical composition of the saturate fraction of Athabasca bitumen by field-ionization mass spectrometry (FIMS), GC, GC/MS, and  $^{13}\text{C}$  NMR.<sup>45</sup> In a near encyclopedic report on the bitumen saturate fraction, sample preparation methods, ionization in mass spectrometry, structural nomenclature, advantageous/short-comings of GC and GC/MS as well as biomarkers are thoroughly discussed. Although not intended as a review, the manuscript provides a wealth of information on bitumen geochemistry, analytical methods, and isolation/purification techniques for saturates. Dutriez and co-workers report the detailed characterization of vacuum gas oil LC fractions (offline) followed by high-temperature comprehensive 2D GC (HT GC × GC) and GC × GC/TOF MS.<sup>46</sup> Expanded compositional analysis of the vacuum gas oil (VGO) is obtained by LC fractionation (ASTM D2007) prior to GC × GC and GC × GC/TOF MS analysis. The LC fractionation permitted the optimization of GC × GC instrument conditions to maximize 2-D resolution for each LC fraction. The optimization facilitated the separation of the *n*-alkanes from the polynaphthalenes (*n*-alkane from alkylcyclohexanes) that were confirmed by TOF-MS through their characteristic fragment ions. The aromatic fraction was analyzed in a similar manner to generate chemical family specific distributions, quantified by carbon number (not boiling point) to optimize the data for kinetic modeling.

**Nitrogen.** Zhu et al. also employed LC fractionation for the increased compositional coverage, in the analysis of coker heavy gas oil by FT-ICR MS.<sup>47</sup> The gas oil was first fractionated by conventional saturates, aromatics, resins and precipitated asphaltenes analysis (SARA) and the isolated resins were subjected to LC separation (six fractions) prior to ESI FT-ICR MS analysis. The resin neutral nitrogen fraction (pyrrolic) displayed a slightly lower molecular weight than the basic nitrogen (pyridinic) species and both were dominated by the N<sub>1</sub> class. Analysis of LC fractions revealed that as the polarity increased, the molecular weight decreased. Dinitrogen species were enriched in the asphaltene fraction and were thought to be amphoteric. GC data were presented in support of the structural evolution of low carbon number species where possible. Al-Hajji et al. analyzed heavy vacuum gas oil (HVGO) and demetallized oil (DMO) derived from Arabian Light crude oil by (+)APPI and ( $\pm$ )ESI FT-ICR MS to highlight acidic, basic, and nonpolar aromatic compositional differences between the two oils.<sup>48</sup> The DMO is found to differ from the VGO in the N- and S-species distribution, where the DMO contains more condensed aromatic species. Interestingly, mono-, di-, and tri-sulfur species were identified in both samples as well as their corresponding acridine and carbazole structural analogues. Li et al. investigated the nitrogen species in different hydrocarbon streams derived from petroleum and coal by GC/MS and GC nitrogen phosphorus detector (NPD) after chromatographic fractionation.<sup>49</sup> Preisolation of the nitrogen compounds (the oxygen-containing compounds as well) facilitated the identification of abundant basic nitrogen compounds in coal derived materials and neutral nitrogen species from petroleum derived streams. Because of

the difference in nitrogen types identified, the implications in denitrogenation processes are discussed. Refinery process issues were also addressed by Wiwel and co-workers in the identification of refractory nitrogen compounds in hydroprocessed VGO by GC/MS, GC coupled with an atomic emission detector (AED), and NMR.<sup>50</sup> The most refractory VGO nitrogen compounds are identified as 4,8,9,10-tetrahydrocyclohepta[*d,e,f*]carbazoles and are confirmed by density functional theory (DFT) calculations. Interestingly, the small structural change upon cyclohepta ring addition predicted by DFT seems to be sufficient to explain the refractory nature of the compound. Mühlen et al. performed a detailed compositional analysis of nitrogen compounds in a heavy gas oil (HGO) by solid–liquid fractionation followed by comprehensive 2-D GC and GC × GC-TOF MS. In a systematic approach, the classification and identification of compounds were performed on seven different categories that include retention times in the first and second dimension, analytical standards coinjection, the structured pattern of separation space, and the structured pattern of separation space with specific *m/z* values.<sup>51</sup> The approach identified more than 100 N-containing species and discusses the use of deconvoluted mass spectra for further compound identification.

**Sulfur.** Lui et al. addressed the selective characterization of sulfide compounds in straight-run diesel and Athabasca bitumen saturate fraction by selective oxidation followed by (+)ESI FT-ICR MS analysis.<sup>52</sup> Methylation for sulfur speciation was revisited by the same authors in an attempt to characterize sulfur species in a Venezuelan crude oil and its SARA fractions by FT-ICR MS.<sup>53</sup> Despite the authors' claim to the contrary, methylation appears to be limited (and selective) in its compositional coverage (i.e., the saturate and asphaltene results lie less than one aromatic ring apart in compositional space and the most aromatic fraction is the resins). However, the highlighted compositional trends as a function of increased heteroatom content and overall compositional coverage of S-containing species are noteworthy. In a continuation of his pioneering work of organosulfur fractionation and characterization, Andersson's group reports the analysis of recalcitrant hexahydrodibenzothiophenes by simple fractionation (no derivatization required) followed by GC/MS and FT-ICR MS. Interestingly, nonaromatic sulfides are tentatively identified ranging from DBE 1–11 and warrant further investigation.<sup>54</sup> In the ever-continuing quest to push GC × GC to higher and higher boiling cuts, Mahé and co-workers present a noteworthy extension of quantitative sulfur speciation to vacuum gas oils with high thermal stability stationary phases in GC × GC SCD and GC × GC-TOF MS.<sup>55</sup> The method facilitates a better (molecular level) understanding of high-boiling sulfur species in hydrodesulfurization processes. Kolbe et al. report the derivatization of phenols to ferrocene esters followed by GC-AED and GC/MS analysis to monitor alkylated phenols (important in stability and lubricity) in desulfurized (conventional and adsorbent methods) gas and diesel samples.<sup>56</sup> Conventional desulfurization was found to lower the phenolic content (especially larger alkylphenols) more effectively than adsorptive desulfurization. In a pair of reports, Heilmann and Heumann developed an isotope dilution GC-ICP MS method for quantification of individual sulfur species<sup>57</sup> and total sulfur<sup>58</sup> in petroleum samples. Both techniques showed excellent agreement with conventional methods in the analysis of low- and high-boiling samples and reference materials.

**Metals.** The challenges to identification and quantitation of metal species in petroleum derived materials were recently reviewed.<sup>59</sup> Soin et al. addressed sample preparation methods

and their effect on ICP MS metal speciation and quantitation.<sup>60</sup> In an important contribution, a collection of researchers reported the speciation of mercury in crude oil by isotope dilution MS and addressed the analysis of extractable and nonextractable Hg species, noting that interconversion among Hg species (especially ethyl-Hg<sup>+</sup> to Hg<sup>2+</sup>) was statistically significant and must be taken into account for accurate speciation.<sup>61</sup> Tonietto et al. presented a HPLC ICP MS method for the determination of Se and As in aqueous refinery streams and eliminated problems associated with Ar dimers through dissociation in a H<sub>2</sub> pressurized octopole.<sup>62</sup> In a pair of reports, Pohl and co-workers eliminated polyatomic interferences with a double-focusing sector instrument (resolution = 4000) for the direct simultaneous determination of 17 metals in organic solutions by ICP MS<sup>63</sup> and laser ablation ICP MS performed off silica thin layer chromatography (TLC) plates, validated by the analysis of standard reference materials.<sup>64</sup> Xie and co-workers presented a similar high-resolution approach for the determination of 20 trace elements in residual oil by ICP MS.<sup>65</sup> Pereira et al. determined metals and metalloids in light and heavy crude oil by ICP MS after microwave-induced combustion (MIC) and used ICP-optical emission spectroscopy (OES) for verification.<sup>66</sup> Polyatomic interferences were eliminated with an ammonia gas reaction cell, and results suggest that MIC allowed a lower limit of detection compared to conventional microwave extraction. Lobinski's group reported on a pair of methods that address multielement molecular size fractionation of oil samples by size exclusion chromatography (SEC) high-resolution ICP MS of Ni and V species,<sup>67</sup> and later on Co, Cr, Fe, Ni, S, Si, V, and Zn.<sup>68</sup> The chromatographic resolution facilitated the identification of at least three classes of Ni and V species and as noted previously, as the high mass resolving power eliminates many polyatomic interferences that allows detailed molecular size element distributions to be determined in petroleum samples.

Qian et al. reported the first direct identification of vanadyl (VO) porphyrins and sulfur-containing vanadyl (VOS) porphyrins in an asphaltene matrix by (+)APPI FT-ICR MS without prior chromatographic fractionation.<sup>69</sup> Importantly, the author report the first identification of sulfur-containing vanadyl porphyrins in an asphaltene sample. Vanyl porphyrins were first identified in a bitumen raw asphaltene and directly detected in unaltered South American crude oil by McKenna and co-workers. On the basis of double bond equivalents (DBE) trends coupled with accurate mass measurements, the authors identified five porphyrin tetra-pyrrolic structural cores and their homologues by (+)APPI FT-ICR MS, noting that DPEP and Etio-porphyrins are the most abundant classes.<sup>70</sup> A follow up (+)APPI FT-ICR MS study by Qian and co-workers reported the first high-resolution mass spectral identification of nickel porphyrins in asphaltenes enriched by a silica-gel cyclograph.<sup>71</sup> The study reports a higher relative amount of highly aromatic (condensed ring structures) nickel and vanadyl porphyrins in more condensed ring structures than previously reported. Therefore, the authors propose kerogen as a potential source of the highly unsaturated, reduced carbon number nickel porphyrins, indicative of porphyrin formation from diagenetic conversion of chlorophylls and corroborate results that agree with previous reports. A recent review by DeChaine and Gray provides a comprehensive review on the analytical techniques and limitations of each method routinely applied to characterize the structure of vanadium compounds in heavy oil, critical for selective removal techniques.<sup>72</sup>

**Naphthenic Acids, Naphthenates, and Neutral Nitrogen.** The analysis of naphthenic acids in environmental samples was recently reviewed<sup>73</sup> and relies on prior derivatization or alternatively, direct characterization by LC–MS or high-resolution mass spectrometry. Rowland et al. describe an amide derivatization method with LC separation followed by MS<sup>74</sup> for structural analysis to reveal bi- to polycyclic acids that contain ethanoate as well as alkyl side chains are abundant in oil sand samples.<sup>74</sup> Fafet et al. employed liquid extraction followed by esterification and subsequent LC–MS analysis for the analysis of biodegraded crudes.<sup>75</sup> The study confirms previous results that suggest the acyclic/cyclic aliphatic acid ratio is directly related to the biodegradation level. Li et al. use derivatization (methyl ester) for GC/MS, FT-ICR, and direct high-resolution FT-ICR MS (without derivatization) for the detailed characterization of high-acidity oils in the Muglad basin (Sudan).<sup>76</sup> Collectively, the techniques reveal differences in the functional groups, chemical classes, and molecular weights of acidic crude components in lacustrine source rocks.

Direct analysis of naphthenic acids by FT-ICR and double-focusing MS was reported by Pötz et al.<sup>77</sup> Comparison of the compositional information provided by both techniques was similar, but the sector instrument was determined to overestimate the relative abundance of high carbon number species due to insufficient mass resolving power. Qian et al. employed low-resolution ESI-MS for the measurement of total acid number (TAN) and TAN boiling point distributions for petroleum samples.<sup>78</sup> The method enabled high-throughput analysis of petroleum samples (via an Advion NanoMate microchip ESI source), and the results agreed well with the conventional titration method. Smith et al. presented the analysis of an Athabasca bitumen and its associated HVGO fraction by (−)ESI FT-ICR MS with and without ion-exchange resin (IER) fractionation.<sup>79</sup> The authors conclude that naphthenic acid distributions may be directly and accurately determined from unfractionated samples and that fractionation affords more detailed compositional analysis of neutral nitrogen compounds due to acid removal. The presence of the SO<sub>2</sub> class in the acid extract and not the acid free fraction strongly suggests the presence of carboxylic acid functionalized thiophenes in bitumen samples. Grewer and co-workers analyzed extractable acidic species from oil sands production water (OSPW) by (−)ESI FT-ICR MS and note that only ~50% of the total abundance could be assigned to conventionally defined naphthenic acids.<sup>80</sup> Thus, ~50% of the total abundance was not “naphthenic acids”. The nature of these unconventional “naphthenic acids” was addressed by Barrow et al. in a combined (±)APPI and ESI analysis of OSPW.<sup>81</sup> Positive APPI FT-ICR MS identified the most species and (−)ESI and APPI revealed similar compositional coverage with an increase in the higher DBE species for APPI over ESI. APPI does offer the additional compositional coverage of nonacidic or basic species (HC and nonpolar S species) unavailable by conventional ESI analysis.

Naphthenate characterization, typically tetraprotic acids commonly termed (ARN) acids, in crude oils and production deposits has been increasingly important as acid rich crude oils are evaluated for production and processing. Its chemical interactions have been studied in aqueous systems<sup>82</sup> as well as ionization efficiency of it and other naphthenic acids by many different ionization methods.<sup>83</sup> Shepherd et al. expanded the ionization study to evaluate derivatization agents for naphthenate studies by TOF MS, GC, 2-D GC, and GC × GC-TOF MS.<sup>84</sup> Silylation chemicals were determined to be the best derivatization

agents for naphthenic acids as BF<sub>3</sub>/MeOH resulted in solubility issues in the presence of ARN acids. Smith et al. evaluated HTGC and HPLC for the analysis of ARN acids and employed ESIMS of individually isolated acids (prep HPLC) to determine their elution order.<sup>85</sup> In the process, they tentatively identified a previously unreported C<sub>81</sub> and C<sub>82</sub> (7 and 8-ring) analogue of ARN acids. Sutton et al. later encountered the same analogues in the LC isolation of 4–8 ringed ARN acids in a detailed description of purification and analysis of ARN acids from a production deposit.<sup>86</sup> APCI and EI MS of the ARN species provide characteristic fragments that are useful for structural determination. C<sub>80</sub> acyclic, mono-, bi-, and tricyclic ARN acids were tentatively identified, and <sup>13</sup>C isotope measurements suggest Archaea bacteria that produce the ARN acids are not involved in aerobic methane oxidation. However, whether the ARN acids in the deposits are a *de novo* biosynthetic product or produced through hydrolysis or oxidation remains unknown. Mapolelo and co-workers published two papers on the characterization of naphthenate deposits (Na and Ca) and naphthenic acid and naphthenate detection in crude oils by ESI FT-ICR MS.<sup>87,88</sup> Sodium naphthenates from different crudes are shown to consist of fatty acids (C<sub>20</sub>–C<sub>35</sub>) with limited contribution from any additional species. Calcium naphthenate deposits were shown to consist solely of ARN acids (C<sub>78</sub>–C<sub>84</sub>) with minor ARN components of lower carbon number C<sub>60</sub>–C<sub>77</sub>. Although a variety of extraction methods were employed, the compositional results were very similar. The compositional analysis of the parent crude revealed species that contribute to sodium naphthenate emulsions could be identified without fractionation. Thus, prediction of potential sodium naphthenate issues can be based on analysis of the parent crude. Fragmentation of ARN acids revealed characteristic water loss and decarboxylation as well as structurally significant alkyl and cycloalkyl loss.

Czarnecki presented the detailed compositional analysis of emulsion interfacial material collected by heavy water and analyzed by FT-ICR MS.<sup>89</sup> The interfacial material is distinct and is different than that of asphaltenes, resins, and the parent oil. Thus, only selected moieties preferentially adsorb at the interface and generalization of the compositional complexity by suggesting that emulsions are exclusively stabilized by asphaltenes is an oversimplification that impedes progress in the field. Stanford et al. revealed the detailed compositional analysis of interfacial material isolated from nine geographically distinct crude oils by FT-ICR MS and demonstrates that regardless of parent oil composition, acidic O<sub>x</sub> and SO<sub>x</sub> species are preferentially enriched in the interfacial material.<sup>90</sup> In contrast, basic species do not preferentially accumulate at the interface by class, type, or carbon number. Freitas et al. analyzed compounds of water-in-crude oil emulsions separated by microwave heating by GC × GC-TOF MS.<sup>91</sup> All samples contained linear hydrocarbons and aromatic, nitrogen, sulfur, and acidic species were identified as well. Muller et al. reported the role of naphthenic acids in emulsion tightness for a low TAN but high asphaltene oil analyzed by FT-ICR MS.<sup>92</sup> A primary group of species that are strongly bound to the water surface is fatty monoprotic and fatty naphthenic/aromatic diprotic acids as well as some alkyl benzene sulfonates. A secondary class of species consists of various classical asphaltene components together with aromatic and naphthenic monoprotic acids.

Neutral nitrogen species were characterized in whole crude oil and its associated LC fractions by (−)ESI FT-ICR MS to reveal their compositional dependent elution behavior.<sup>93</sup> The LC technique produced a low yield of carbazole in the neutral

## Positive Ion APPI FT-ICR MS of VBR Asphaltenes from Heavy Crude Oil

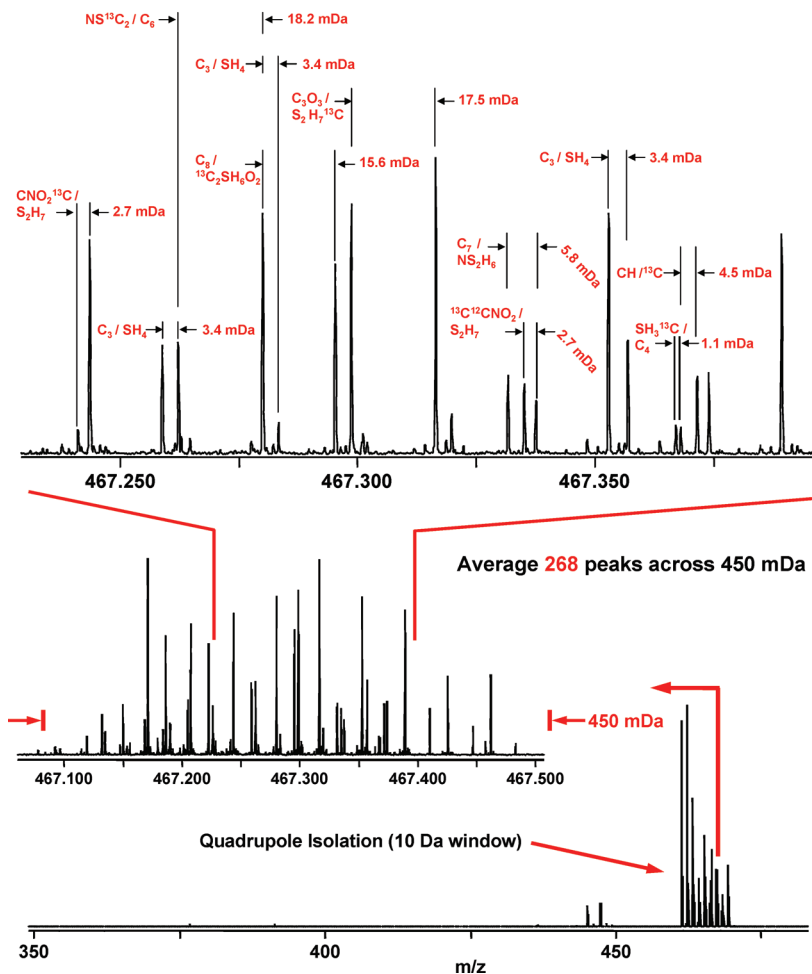


**Figure 1.** Positive-ion atmospheric pressure photoionization (APPI) 9.4 T FT-ICR mass spectrum of asphaltenes fractionated from vacuum bottom residue of heavy crude oil. Quadrupole mass isolation significantly improves the dynamic range, since only ions with mass-to-charge ratios within a narrow mass range ( $\sim 10$  Da) are accumulated and transferred to the ICR cell for detection. The extreme compositional complexity of asphaltenes can clearly be observed, with more than 250 mass spectral peaks detected across a 450 mDa mass window. Isobaric overlaps, species with the same nominal mass but different exact masses, of some common mass splits observed for asphaltenes/heavy crudes are highlighted. Three important close mass doublets are molecules whose elemental compositions differ by  $^{12}\text{C}_3$  versus  $^{32}\text{SH}_4$  (3.4 mDa),  $^{13}\text{C}$  versus CH (4.5 mDa), and  $\text{SH}_3^{13}\text{C}$  versus  $\text{C}_4$  (1.1 mDa) for accurate elemental composition assignment and require the ultrahigh resolving power of FT-ICR MS.

nitrogen fraction, which was enriched in low molecular weight species. Low DBE, high carbon number species eluted in the aromatic fraction, many of which were not detected in the analysis of the whole crude. Surprisingly, a portion of the neutral nitrogen species eluted in the amino fraction, thus caution was recommended when the LC method is used due to previously overlooked analytical bias. Shi described the detailed molecular composition of a Chinese crude oil, its distillate fractions and residue by (-)ESI FT-ICR MS.<sup>94</sup> Detailed compositional results reveal the progression of naphthenic acids and neutral nitrogen species as a function of boiling point. The authors note the presence of hopanoic acids and sterol-like compounds that are assumed to be the major contributors to TAN. The authors also presented a similar study on the characterization of heteroatom compounds in oil, SARA, and neutral nitrogen fractions by FT-ICR MS.<sup>95</sup> The analysis reveals the compositional differences and similarities of the crude and isolated fractions in heteroatom compound distributions, type, and carbon number.

**Asphaltenes.** Direct asphaltene characterization is difficult for a number of reasons. First, characterization of asphaltenes by conventional ionization methods requires efficient desolvation/ionization of all asphaltene components, a challenge due to the high boiling point and solubility limitations of this solubility defined fraction of crude oil. Second, asphaltene compositional diversity is at least 10-fold higher than that of the maltene fraction and therefore requires ultrahigh mass resolving power (>500k at  $m/z = 500$ ), only obtainable by FT-ICR MS (see Figure 1). Third, asphaltenes are known to self-associate at very low (ppb) concentrations, a concentration well below that required for most mass spectral techniques. Thus, asphaltenes are present as nanoaggregates (not monomers) in all atmospheric pressure ionization and laser based ionization reports.

**Asphaltene Molecular Weight.** The controversy over asphaltene molecular weight has been extensively highlighted in the literature.<sup>96</sup> The ultrahigh-resolving power of FT-ICR MS can separate asphaltene species and naturally lends itself to complex

asphaltene sample characterization. The Kenttämaa group demonstrated molecular ion formation for a series of asphaltene model compounds and asphaltene samples to address asphaltene molecular weight by LIAD-EI/FT-ICR MS and reported an asphaltene molecular weight range from 350 to 1050 Da with little to no fragmentation.<sup>97</sup> Surprisingly, the authors conclude that the lack of low mass fragments (even at high electron energies) suggests the molecular asphaltene ions are stabilized by the presence of long alkyl side chains.

**Asphaltene Composition/Structure.** Laboratory-generated deposits that simulate reservoir conditions are critical test beds to understand deposition mechanisms. Organic solid deposition control (OSDC) generates deposits on live crude oil under production system conditions and different gas loads, helpful in production of low-energy reservoirs. Comparison of the molecular composition of OSDC deposits with different gas loads to asphaltenes precipitated from the same parent crude provides a method to mimic reservoir deposit formation in the laboratory for further interrogation. Juyal and co-workers presented the first compositional characterization of OSDC deposits under gas lift conditions and compared polar species within each deposit to the parent crude by ( $\pm$ )ESI FT-ICR MS.<sup>98</sup> The authors observed enrichment in the relative abundance of acidic species in OSDC deposits relative to the parent crude, in particular  $O_x$  and  $S_xO_y$ , implicated in multiple production problems (mostly deposit formation) due to its high polarity. Surprisingly, the effect of two asphaltene inhibitors under OSDC conditions suggests the molecular structure of the inhibitor itself could contribute to deposition in the parent crude. Smith et al. examined oil-specific chemistry for two asphaltene inhibitors and asphaltenes derived from two geographically distinct crude oils and parent crudes to characterize the polar species by ( $-/+$ )ESI FT-ICR MS and presented the first evidence that inhibitor effectiveness relates to heteroatom content and polar composition of the crude.<sup>99</sup> Although two crudes had similar TAN values, polar molecular speciation dictated the oil-inhibitor chemistry and inhibitor effectiveness, an important tool for development of effective inhibitors. Conversion processes for asphaltenes rely on deep hydrotreatment processes, which can differ in the degree of severity and quickly lead to coke formation. Purcell and co-workers characterized the molecular evolution of the hydrocarbon and sulfur families in asphaltenes during deep hydrotreatment processes under different degrees of severity by (+)APPI FT-ICR MS.<sup>100</sup> The authors reported a drastic reduction in the chemical polydispersity with increasing extent of desulfurization although sulfur species remain compositionally similar. Interestingly, the hydrocarbon class exhibits a drastic increase in aromaticity with process severity, reported as highly condensed dealkylated aromatic structures, indicative of possible coke formation.

**Geochemistry.** Advances in reservoir characterization were demonstrated by Mullins et al. in a combined visible-near-IR spectroscopy downhole fluid analysis (DFA) probe and subsequent comprehensive 2-D gas chromatography and 2-D GC  $\times$  GC TOF MS (on captured samples) analysis to address oil reservoir architectural complexity.<sup>101</sup> In situ analysis of petroleum fluids by the DFA probe facilitates the identification of compositional gradients within an oil column and discontinuous changes in fluid properties (to identify flow barriers and thus, compartments). Samples collected by the DFA probe allow for further characterization by high-resolution mass spectrometry<sup>102</sup> or in this case, GC  $\times$  GC, which highlights compositional

changes in captured petroleum fluids at different vertical well depths. Here, quantitative changes in compound classes revealed by GC  $\times$  GC analysis are visualized by a spider diagram that highlights changes in steranes, hopanes, normal and branched alkanes, linear and substituted alkylbenzenes, and substituted naphthalenes and phenanthrenes currently difficult to obtain/unavailable by GC/MS or ultrahigh-resolution MS. Bentancourt and co-workers expanded on the previous DFA work to show that asphaltenes in a 658 ft vertical column of oil exhibited gravitational sedimentation consistent with the presence of asphaltene nanoaggregates with a size of  $\sim 2$  nm.<sup>103</sup> The results strongly suggest that asphaltenes are present in the reservoir as nano-colloids. An equation of state (EoS) analysis of asphaltenes with literature constants and molecular weights yields an aggregation number of  $\sim 8$ . As with the previous studies, GC  $\times$  GC and high-resolution FT-ICR MS results establish the similarities between the collected oil samples and assess potential levels of biodegradation. Pomerantz et al. recently presented a continuation of the work with a combined DFA, GC  $\times$  GC and FT-ICR MS analysis to address reservoir connectivity.<sup>104</sup> Detailed compositional analysis suggested the reservoir experienced multiple charges and contains a mixture of oils that are different in the extent of biodegradation. The initial charge is implicated in a disproportionate contribution to asphaltene content due to early biodegradation.

Tran et al. presented a GC  $\times$  GC TOF method to compare compositional changes in biodegradation in land/plant, marine and mixed land/plant–marine oils.<sup>105</sup> Advantages in reversal of the conventional nonpolar/polar (NP/P) column to a polar/nonpolar (P/NP) configuration are highlighted for resolved and unresolved complex mixture (UCM) components that include, in part, diamondoids, biomarkers, alkanes, and aromatic hydrocarbons. Prominent UCM components identified in all three oil types are similar and comprise isomers of alkyl-decaphenylanes ( $C_1$ – $C_7$ ). Wei et al. expanded the knowledge of diamondoids with the first report of the natural occurrence of higher thiadiamondoids and diamondoidthiols in a deep petroleum reservoir offshore Mobile, AL, by GC-SCD, GC/MS, and GC  $\times$  GC-TOF MS.<sup>106</sup> Nonsulfurized diamondoids (1–6 cages) are accompanied by their sulfurized structural analogues and attributed to thermochemical sulfate reduction (TSR) in deep, hot reservoirs. The GC  $\times$  GC-TOF MS results consistently indicate the occurrence of open-cage diamondoidthiols that may function as a reaction intermediate in thiadiamondoid synthesis, since sulfur cannot directly replace carbon in diamondoids due to their high stability. TSR is further implicated in higher thiadiamondoid synthesis by sulfur isotopic data, thus they can be used as molecular indicators of TSR and subsequent sour gas production. Springer and co-workers used diamondoids and biomarker ratios collected from the GC/MS analysis of 22 oils from a Columbian sedimentary basin to provide a more refined maturity assessment since most of the oils in the sample set were biodegraded.<sup>107</sup> The ratios were used to distinguish different levels of thermal maturity and consider possible mixtures of oils from distinct generation/migration pulses. Sharipova et al. performed a similar analysis of 120 chloroform extracts of sedimentary rocks from Middle and Upper Devonian deposits that focused on the peak areas associated with polycyclic biomarkers.<sup>108</sup> Correlations between the types of organic matter (OM) and their associated concentration of polycyclic hydrocarbon biomarkers allow differentiation of the OM with respect to the age and thermal maturity. Aguiar and co-workers found it necessary to employ GC  $\times$  GC-TOF MS for the identification of methylhopanes in Brazilian oils due to their

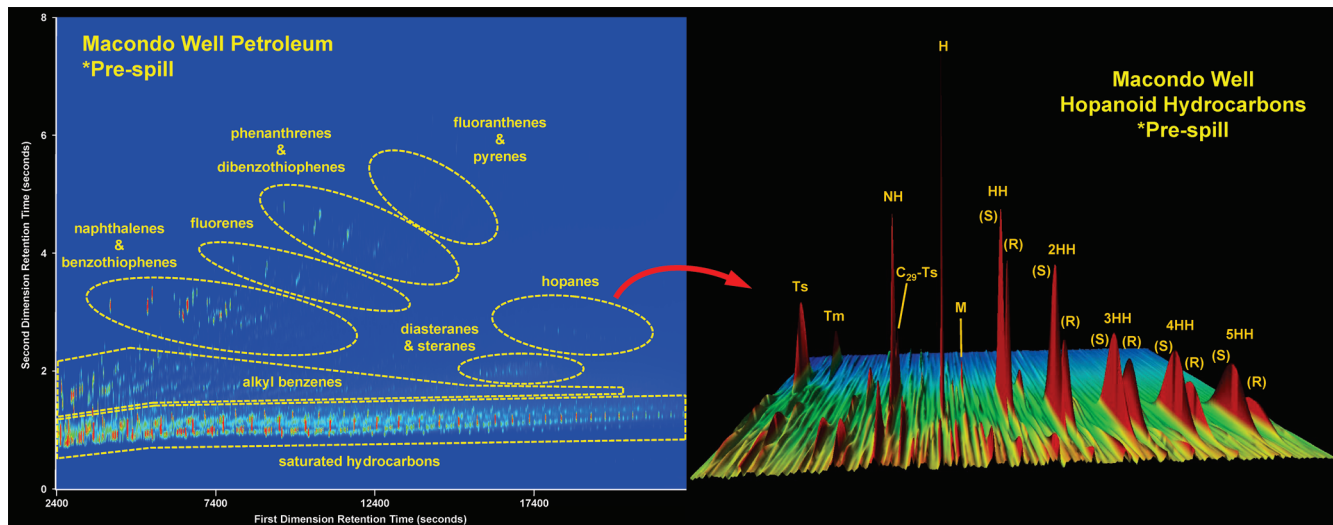


**Figure 2.** GC  $\times$  GC chromatogram of whole light crude oil from the Gulf of Mexico with distinct chemical classes highlighted (left) and zoom inset of the diasterane/steranes biomarker region (right). The data is displayed as color-contour plots, with blue representing low signal, white representing medium signal, and red representing high signal. A volatility-based separation produced a boiling point separation on the  $x$ -axis and a polarity-based separation on the  $y$ -axis. The whole crude oil (left) was collected from the broken riser from the Deepwater Horizon well and was analyzed without prior fractionation. Thus, naphthalenes, fluorenes, phenanthrenes, and pyrenes are observed, which are removed in silica gel fractionation routinely performed prior to GC  $\times$  GC analysis. For the diasterane/steranes chromatogram (right), the Macondo well oil sample was fractionated, and the hexane-soluble material not retained by the silica gel (F1 fraction) was analyzed. Silica gel fractionation prior to GC  $\times$  GC analysis permits the length of the second dimension to be shortened, thereby increasing resolution in the first dimension. The authors graciously thank Christopher M. Reddy and Robert K. Nelson from Woods Hole Oceanographic Institute for providing GC  $\times$  GC data and the figure.

insufficient separation in GC/MS.<sup>109</sup> They tentatively identified a novel terpane series ( $C_{30}$ – $C_{34}$ ) that eluted after the regular hopanes, as well as bis-norgammacerane and a pair of homohopanes. The authors suggest the presence of methylhopanes may indicate oxygen-producing cyanobacteria were important biological inputs in the deposition environment.

Ávila et al. employed GC  $\times$  GC-TOF MS for biomarker identification in extra heavy gas oil (EHGO) that facilitated the resolution and identification of many coeluting compounds such as tricyclic and pentacyclic terpanes.<sup>110</sup> Although demonstrated largely for biomarker characterization, the increased compositional information afforded by GC  $\times$  GC-TOF MS is offered as a method for distillate cut evaluation to guide the selection of refinery conversion processes. Compound-specific stable carbon isotope analysis (CSIA) by gas chromatography-isotope ratio mass spectrometry (GC-IRMS) of *n*-alkanes from Columbian oil samples allowed differentiation between Cretaceous and Cretaceous/Tertiary oil samples.<sup>111</sup> The heavier isotope composition is attributed to their major terrigenous organic matter input and confirms that the oils have both marine and terrigenous-derived organic matter inputs that reflect the deposition environment. In a combined FT-ICR MS, GC  $\times$  GC, and 2-D fluorescence spectroscopy analysis of an unusually blue crude oil, perylene was identified as the source of the oil's blue color.<sup>112</sup> The oil was responsible for deposition issues experienced in a monoethylene glycol (MEG) regeneration unit on an offshore production platform. FT-ICR MS analysis of the deposit reveals that it is compositionally enriched in hydrocarbon ( $C_{27}$ – $_{32}$ ) species with a DBE (double bond equivalents or rings + double bonds) of 5–9. The species are suspected to be polycyclic biomarkers and is supported by (−)ESI FT-ICR MS analysis of the crude oil and deposit that shows a commensurate increase in naphthenic acid species (hopanoic acids) of similar carbon

number and DBE. Clinching evidence is provided by GC  $\times$  GC and GC  $\times$  GC-TOF MS analysis that confirms the enrichment of biomarkers and identifies the structural isomers not provided by the FT-ICR MS data (as demonstrated for the now infamous Deepwater Horizon Macondo well crude oil, see Figure 2). 2-D fluorescence unequivocally identifies perylene as the source of the unusually blue oil, which is supported by both GC  $\times$  GC and FT-ICR MS data. Simoneit et al. report the characterization of another unusual oil from Kamchatka by GC/MS and accelerator mass spectrometry (AMS). The GC/MS results suggest the oil originates from the hydrothermal alteration of algal and bacterial detritus and not from higher plants. The AMS data reveals that it has a  $^{14}\text{C}$  age of approximately 1000, a BP, and a  $\delta^{13}\text{C}$  value (−30.6%) typical of biosynthesis. Thus, the oil is the youngest hydrothermal petroleum reported to date and not evidence of abiotic Fischer–Tropsch type oil synthesis.<sup>113</sup>

Pyrolysis of asphaltenes followed by GC/MS has been applied to probe asphaltene molecular structure for more than 30 years, with early reports in the early 1980s. Pyrolysis of asphaltenes fractionated from two crudes of different geological origin followed by GC/MS was applied to assess thermal maturity based on the ratio of stable  $\beta$ -substituted to less stable  $\alpha$ -substituted isomers of alkylnaphthalenes and alkylphenanthrenes.<sup>114</sup> Both asphaltene pyrolysates exhibited higher relative concentrations of 1-methylphenanthrene over 9-methylphenanthrene, both less stable  $\alpha$ -substituted isomers, an indication that both parent asphaltenes were terrestrial in origin. In a similar study, asphaltene pyrolysates from three crude of different geological origin were characterized based on pyrolysis (Py) GC/MS and IR spectra.<sup>115</sup> On the basis of *n*-paraffin distributions obtained by Py-GC for asphaltenes, parent crude, and kerogen, the authors conclude that asphaltenes are the smallest group of kerogens that can produce hydrocarbons through geochemical evolution.

## ■ SEPARATIONS

The compositional diversity inherent to fossil fuels limits the direct applicability of most analytical techniques and many researchers apply separation techniques, including chromatography, fractionation, and solubility-based separations prior to analysis. Some techniques are applied to separate and determine individual compound types, chemical moieties, or structural motifs. Barman and Cebolla et al provided a comprehensive review of developments in chromatographic techniques in 2000 for the separation and quantitative characterization of petroleum and related products.<sup>116</sup> The next section will detail recent advances in separative techniques applied to petroleum characterization.

## ■ RECENT ADVANCES IN GAS CHROMATOGRAPHY

Gas chromatography (GC) separates volatile components of mixtures through a chromatographic fraction with a gaseous mobile phase. Because GC separations are highly efficient, with columns equivalent to 1 000 000 theoretical plates, it is ideally suited to the quantitative analysis of mixtures of known components and the preferred technique for the analysis of petroleum gases in refinery applications. GC analysis of heavier petroleum requires prior separation techniques to reduce complexity due to low volatility and isomeric coelution, which limits GC applications to lighter distillates.

**Paraffins and Waxes.** One of the most important contributors to flow assurance problems is paraffinic wax precipitation and routine thermodynamic models (wax precipitation curve, WPC) require molecular weight and *n*-paraffin distributions, typically determined by high-temperature gas chromatography (HTGC). However, *n*-alkane quantification is limited based on low signal-to-noise ratios, incomplete elution of heavy paraffins, and baseline changes across the chromatogram. Several studies by Pena and co-workers have sought to overcome the limitations associated with HTGC determination of wax precipitation. An early method based on multistage wax fractionation by decreased temperature eliminates solvent effects and obtains wax appearance temperature (WAT) for two chemically different crudes.<sup>117</sup> A more recent method developed by the same group includes fluid composition and solid–liquid equilibria based on a simplified thermodynamic model and yields the wax appearance temperature, full wax precipitation curve, and estimated wax composition.<sup>118</sup> This method based on a differential scanning calorimetry (DSC) introduces a simplified, rapid method to determine the WAT and WPC and experimental conditions optimized for several crude oil cuts from a naphthenic crude oil. A recent advancement explores three variables to improve *n*-paraffin distributions obtained by HTGC and studies the amount of  $C_{20}^+$  paraffins, extrapolates heavy *n*-paraffins from  $C_{38}^+$  to overcome HTGC limitations, but requires a fit with WAT obtained by differential scanning calorimetry (DSC) for reliable wax content.<sup>119</sup> Methods for extraction and characterization of waxes from crude oils was recently evaluated by Espada et al.<sup>120</sup> Coto et al. reported reliable *n*-paraffin distributions obtained for saturates from two fractionation techniques and whole crudes based on HTGC and DSC analyses improves signal-to-noise limitations and highlights the importance of accurate *n*-paraffin distributions for correct prediction of WPC based on thermodynamic models.<sup>121,122</sup> Martos et al. further investigated improvements to *n*-paraffin distributions determined by HTGC and compared WPC measurements obtained by  $^1\text{H}$  NMR and DSC and explores discrepancies between experimental and predicted WAT and WPC.<sup>122,123</sup>

**Nitrogen.** Nitrogen species have been implicated in catalyst fouling, corrosion, and storage instability. A recent method developed by Li et al. provides identification and quantification of nitrogen compounds in routine hydrocarbon streams derived from petroleum and coal combines modified solid phase extraction (SPE) and GC/MS and nitrogen/phosphorus detector (GC-NPD) for deep hydrodenitrocification.<sup>49</sup> This method compared nitrogen species in petroleum and coal-derived streams and concluded that pyridinic nitrogen were the major nitrogen structure in coal, whereas pyrrolic nitrogen were dominant in petroleum feeds, important for accurate denitrification process optimization. A further study by Wiwel et al. combined SPE, GC/MS, GC-AED, and NMR to characterize nitrogen compounds in severe hydrocracking feeds.<sup>50</sup> Importantly, this method determined the most refractory organic nitrogen species introduced to the hydrocracker belong to the family of 4,8,9,10-tetrahydrocyclo-[def] carbazoles, a basic form of carbazole implicated in downstream catalyst poisoning. Persistent nitrogen species in middle distillates after catalytic filtration was characterized by GC/MS again determined recalcitrant nitrogen species were dominated by pyrrolic nitrogen.<sup>124</sup>

**Pyrolysis GC.** Pyrolysis and subsequent GC/MS of asphaltenes, crude oils, and kerogens revealed trends in *n*-alkane distribution patterns that concluded the crude oil and asphaltenes originated from the same source rock and that asphaltenes were unconverted forms of parent kerogen.<sup>115</sup> The authors characterized the interfacial and thermal behavior of asphaltenes fractionated from crudes of different origin with FT-IR spectroscopy, interfacial tension measurement, thermogravimetric analysis, and pyrolysis gas chromatography mass spectrometry (Py-GC/MS). Thermal maturation indicators, such as alkynaphthalenes and alkylphenanthrenes, have been reported in pyrolysates of asphaltenes from crude oils of different origin by pyrolysis GC/MS. However, Py-GC/MS still lacks the chromatographic separation power required for reproducible, semiquantitative analysis. Consequently, Wang and Waters introduced pyrolysis GC × GC (Py-GC × GC) with sulfur specific detection/flame ionization detector (FID) for the characterization of petroleum source rocks and provide enhanced quantitative compositional information through enhanced chromatographic separation.<sup>125</sup> The authors apply detailed molecular fingerprints to better understand the relationship between kerogen composition, deposition environment, thermal maturation, and biotic input.<sup>125</sup> Py-GC × GC systems are more robust, cheaper, and automated than conventional Py-GC/MS systems and provide reproducible, quantitative analysis with afforded enhanced chromatographic separation. Five source rocks were characterized by Py-GC × GC and the resulting chromatograms compared to Py-GC/MS. Importantly, all geochemical parameters by conventional Py-GC may be measured by Py-GC × GC, but minor components (usually measured by MS) are quantified in a single Py-GC × GC analysis. For example, the ratio of prist-1-ene to  $C_{17}$  is measurable by Py-GC/MS, but hopanes/steranes ratios require target compound analysis by MS; however, ratios may be measured from a single Py-GC × GC-FID analysis.

## ■ SIMULATED DISTILLATION

The distribution of distillation temperatures and yields in petroleum crude oil provides indispensable information for petroleum industries to determine effective processing conditions for refinery feeds. This parameter provides valuable

information on crude oil type and content of individual fractions, classifies in terms of boiling points, and provides optimum conditions and effectiveness of separation into fractions of atmospheric and vacuum distillation. Physical distillation methods (such as ASTM D86, D1160, and D2892) resemble refinery operations but are time-consuming and cost prohibitive for routine process control.

## ■ COMPOSITION-EXPLICIT OR ADVANCED DISTILLATION CURVE

Classical distillation curves are typically represented by graphical depiction of boiling temperature of the mixture plotted against the volume fraction distilled, typically depicted as cumulative percent of the total volume. However, standard assay types do not provide saturated bubble temperatures and require conversion into true boiling point data. Recently, Bruno et al. introduced the composition-explicit or advanced distillation curve (ADC) and provided a review of the distillation curve methodology and application to complex fluids.<sup>126,127</sup> Here, measured distillation temperature corresponds to a true thermodynamic state point through careful placement of the thermometer in the boiling fluid and instantaneously measuring bubble temperatures and allowing for measurement of compositions. This method has been applied to a wide variety of mixtures and facilitated a consistent thermodynamic model for biodiesel.<sup>127–130</sup> A new method investigates replacement of current SimDis columns with deactivated fused silica capillary phase without any stationary phase to allow lower elution temperature (decrease final oven temperature) but still results in a complete separation for high-boiling petroleum fractions.<sup>131</sup>

The Yarranton group investigated limitations of utility of the ADC and ASTM D5236 for heavy hydrocarbon characterization, where both methods obtain measured temperatures with precise thermodynamic meaning.<sup>132</sup> The authors proposed a simple, general characterization procedure for advanced distillation curves that divides crude oil into pseudocomponents and determines their mole fraction based on distillation data from ADC assays. A methodology based on previously published mathematical modeling for ASTM D5236 by Eckert and Vanek to determine what initial composition of pseudocomponents for a particular fluid corresponds to the same trajectory of measured temperature versus volume of material distilled. Importantly, this novel method is not based on any specific thermodynamic model and therefore can be applied to the compositional analysis of distillation of any material. Here, successful thermodynamic models were developed for bitumen and coupled with previous methodologies to estimate distillation curves for heavy hydrocarbons.

## ■ MULTIDIMENSIONAL GAS CHROMATOGRAPHY

One of the most powerful and actively growing petroleum applications is analytical techniques of two-dimensional gas chromatography. Wang et al. recently reviewed the widespread application of comprehensive two-dimensional gas chromatography.<sup>133</sup> Compared to conventional 1D-GC, GC × GC exhibits enhanced peak capacity due to multiple separation dimensions and achieves high sensitivity due to analyte compression between separations.

## ■ TARGETED MULTIDIMENSIONAL GAS CHROMATOGRAPHY

Classical multidimensional gas chromatography (MDGC) collects discrete heart cut fractions from a first dimension column

to a second column for improved separation for target eluants. Here, eluents from selected regions of a primary chromatogram are further separated on a secondary column.<sup>134</sup> Recent development of the switchable MDGC/GC × GC system permits independent operation of GC, GC × GC to targeted MDGC multiple times through a single analysis and has been applied to complex essential oil mixtures, shows significant promise for improved separation for targeted regions, and retains compositional information of the samples from GC × GC separation in one system.<sup>134</sup> A novel preparative technique based on capillary multidimensional gas chromatography separated 1- and 2-methylnaphthalene isomers from crude oil with enough quantity for NMR confirmation.<sup>135</sup>

## ■ COMPREHENSIVE TWO-DIMENSIONAL GAS CHROMATOGRAPHY (2D-GC OR GC × GC)

Comprehensive two-dimensional gas chromatography with flame ionization detection (GC × GC/FID) applied to assessment of oil contamination in environmental samples surpasses typical GC-based methods, such as standard total petroleum hydrocarbon (TPH) measurements and revolutionized environmental crude oil analysis.<sup>136,137</sup> GC × GC has been applied to study several oil spills to account for weathering, evaporation, dissolution, and degradation of oil in the environment and for source identification.<sup>138–141</sup> Natural hydrocarbon sources, such as petroleum seeps, have been extensively characterized by GC × GC.<sup>105,142,143</sup>

**Industrial Applications of GC × GC.** The application of GC × GC as an industry-accepted analytical method requires further developments to improve robustness, ease of use, flexibility, and instrument portability. Wang reported a new design for a valve switching modulation system for comprehensive two-dimensional gas chromatography based on differential flow easily installed on most gas chromatographs that can support a wide range of stationary phases for improved flexibility of the system to petroleum applications.<sup>144</sup> Van Geem et al. introduced the first setup for online qualitative and quantitative comprehensive GC × GC-FID/TOF-MS for hydrocarbon mixtures in a single apparatus and extends capabilities to routine industrial processes.<sup>145</sup> Polar organic compounds, implicated in corrosion and related refinery problems, were tentatively identified for the first time in organic acid extracts through a microwave extraction method followed by GC × GC-TOF-MS.<sup>91</sup> Until recently, comprehensive multidimensional chromatography applications have been limited to middle distillate fractions due to temperature limitations of polar columns and modulation problems at the desorption step. In 2009, conditions based on high-temperature conditions with an adapted modulation step extended the application of GC × GC to the vacuum gas oil (VGO) boiling range<sup>146</sup> and demonstrated the applicability to a wide range of heavy VGOs.<sup>147,148</sup>

**Nitrogen.** Similarly, nitrogen compounds implicated in catalyst poisoning were identified by GC × GC coupled with nitrogen-specific detection (NCD) to characterize basic/neutral nitrogen compounds in diesel feedstock, similar to earlier work by Wang, Greaney, and Robbins.<sup>149</sup> Nitrogen-containing compounds were characterized in heavy gas oils with a solid–liquid fractionations scheme coupled with GC × GC-TOFMS.<sup>51</sup>

**Sulfur.** The first report of naturally occurring higher thiadiazidines and diamidothiols in a gas seep from a petroleum reservoir utilized GC/MS, GC-SCD, and GC × GC-TOF MS to

identified several isomers, although their geochemical origin remains unknown.<sup>106</sup> High-temperature GC × GC-SCD was applied for the first time to the characterization and quantitation of sulfur species in VGOs and introduced a new method for sulfur speciation in heavy petroleum cuts.<sup>55</sup>

## SUPERCRITICAL FLUID CHROMATOGRAPHY AND EXTRACTION

Supercritical fluid chromatography (SFC) combines both gas and liquid properties of a supercritical fluid and enables the elution of higher molecular weight materials, since the mobile phase has the low viscosity of a gas and the variable solvent strength of a liquid. Therefore, SFC is often applied to compounds too heavy to meet volatility requirements for GC. Supercritical fluid extraction (SFE) is a nonchromatographic technique where a sample is extracted under supercritical conditions and successive fractions are obtained through gradual variation of pressure that adjusts the solvent strength. Zhang et al. separated a vacuum residue into 16 extractable fractions and 1 nonextractable end cut by SFEF and further separated all fractions into SARA subfractions.<sup>150</sup> The chemical structure of the parent VR, end cut, and subfractions was investigated through RICO and postulated the predominance of polymethylene bridges between multiple aromatic cores for heavy crude oil fractions.

A recent method developed by Sjöblom et al. extracts the basic molecules from petroleum in significant amounts based on cation-exchange sorbent recovered with methylamine.<sup>151</sup> Importantly, this method produces efficient extraction yields between 70 and 90% for bases from four crudes, from light crude to extra-heavy crudes, and correlates with elemental analysis and total base number titration methods. The quantitation and repeatability of this method provides a method to extract yields of basic components (700 mg) sufficient to investigate physical and chemical properties. A follow-up study applied the extraction technique to study surface and interfacial properties in oil/water systems to determine their role in water-in-oil emulsions.<sup>152</sup> Similarities between isotherms from extracted basic and maltene fractions correlates with previous work that concludes the majority of basic species are a subfraction of maltenes, important in emulsion stability.

## SIZE-EXCLUSION CHROMATOGRAPHY

Size exclusion chromatography (SEC), or gel permeation chromatography (GPC), separates by molecular size independent of chemical composition. Molecular size (hydrodynamic volume) relative to the pore size of the stationary phase determines retention in SEC, and elution is determined by total exclusion or total permeation.<sup>116</sup> Although a low-resolution technique which often results in broad and continuous elution profiles for petroleum, SEC has been used to obtain molecular weight distributions of heavy crude oil fractions and asphaltenes.<sup>153,154</sup> However, SEC measurements have been criticized for molecular weight determination of heavy ends and asphaltenes due to lack of appropriate calibrants, packing materials, and solvents.<sup>96,155</sup> Several groups have attempted to explain the bias in SEC measurements for asphaltene molecular weight determinations. In 2008, Trejo and Ancheyta applied SEC fractionation with THF as a solvent to solubility fractions of asphaltenes to investigate the molecular weight distribution of asphaltenes from hydrotreated crude but acknowledge the solvent bias inherent to SEC.<sup>156</sup> SEC with element specific detection with inductively coupled plasma atomic emission

spectrometry (SEC-ICP-AES) is routinely applied to determine vanadium, nickel, and sulfur as a function of molecular weight.<sup>67</sup> Recently, Pohl et al. developed a method to evaluate a wider range of components by optimization of the coupling of size exclusion microchromatography with a high-resolution mass spectrometer.<sup>68</sup>

Heavy oil subfraction methods based on sequential elution fractionation (SEF) after distillation first developed by Boduszynski et al. have been recently developed that allow for correlation between subfractionation of heavy oil and viscosity reduction, critical for heavy oil processing.<sup>153,157</sup> To the best of our knowledge, there have been no recent applications of SEF to characterize heavy petroleum cuts or asphaltenes.

## CAPILLARY ELECTROPHORESIS (CE)

Capillary electrophoresis (CE) has routinely been used to characterize and separate charged species in solution, and the method and instrumentation has been reviewed by Kok extensively in the literature. Ionic compounds are separated in capillaries filled with a background electrolyte and separation occurs through size or charge differences and results in differences in electrophoretic mobility. Deposition tendencies for crude oil are thought to correlate with charge speciation of aggregated molecules, such as asphaltenes, present in the native crude. However, the majority of CE applications utilize an aqueous background electrolyte, problematic for crude oil samples. Recently, nonaqueous CE has increased in application for solutes which are not readily water-soluble and was reviewed by Geiser and Veith in 2009. A recent novel method for investigation of the charge properties of asphaltenes with nonaqueous CE was developed by Kok et al. and solvent mixtures optimized for asphaltene solubility and solution electrical conductivity.<sup>158</sup> The optimized method was applied to asphaltene field deposits and SARA fractions from three unstable crude oils to better predict deposition tendencies and mechanisms. Preliminary results indicate that the asphaltene field deposit was composed of two major fractions, a neutral fraction and a positively charged fraction. Unstable crude oils, known to cause deposition, shared similar charge distributions, which differed from the stable crude oil and further studies to determine the applicability of the technique to downhole analysis to predict deposition. Capillary electrophoresis (CE) was used to separate polycyclic aromatic sulfur heterocycles in diesel after catalytic hydrodesulfurization (HDS) to determine the amount and functionality of recalcitrant sulfur-containing compounds after derivatization but required a preconcentration step for UV detection.<sup>159</sup> Characterization of sulfur species which remain after deep HDS is critical for optimization of refinery processes to remove sulfur compounds to meet stringent government standards for sulfur quantities in gasoline and diesel fuel.

## HIGH-PERFORMANCE LIQUID CHROMATOGRAPHY

The compositional diversity of petroleum and its fractions leads many researchers to detailed separative techniques prior to analysis.<sup>125</sup> High-performance liquid chromatography (HPLC) separates individual components of petroleum and partial identification of compound classes. Robbins developed the first high-performance liquid chromatography (HPLC-2) system for quantitative measurement of the distribution of aromatic carbon and mass in heavy petroleum distillates, which separates based on ring number.<sup>160</sup> A critical analysis of the application of HPLC in

group-type analysis of petroleum products was conducted by Kaminski et al.<sup>161</sup> Oro and Lucy introduced a hypercrosslinked polystyrene stationary phase to separate nitrogen groups into pyrrole (five-membered ring) and pyridinic (six-membered ring) fractions in a recent application of HPLC in quasi-normal phase (QNP).<sup>162</sup> The rigid, hypercrosslinked stationary phase contains alkyl-linkages between the phenyl groups of polystyrene and is devoid of polar groups and, therefore, specific adsorption sites on the surface. This method showed the best selectivity for nitrogen group-types and polycyclic aromatic hydrocarbons with a separation under gradient conditions in less than 30 min, much faster than previous methods. Tomic et al. proposed a method to determine alkene content in fluid catalytic cracking products by normal-phase HPLC with diode array detection and utilized an amino-modified silica gel column with *n*-heptane as the mobile phase with UV-diode array detection (UV-DAD).<sup>163</sup> Here, the column has slight affinity to alkenes and saturated hydrocarbons but a pronounced affinity to aromatic compounds. Coelution of alkenes and saturates is typically problematic on silica gel; however, UV-DAD is sensitive and selective to alkenes, and saturates are inactive in the UV field. Alkene contents were quantified with high correlation coefficients with good reproducibility, and the method was validated with NMR. Barth and co-workers introduced a normal phase HPLC procedure with a cyanopropyl bonded phase column to separate organic acids from crude oil<sup>164</sup> and applied the technique to acid extracts from biodegraded crude oils to investigate hydrate formation.<sup>165</sup> This method has been developed as an analytical tool for characterization of acid extracts as well as a preparative-scale technique, important for complementary method characterization. Remediation of oil-contaminated sediments requires characterization of the oil composition and physical/chemical processes; therefore, petroleum hydrocarbons have been analyzed extensively by GC × GC. However, GC × GC still suffers from incomplete separation of hydrocarbons. A novel method applied HPLC with a silver-modified column was first introduced as a prefractionation technique coupled with GC × GC (HPLC–GC × GC) to improve chemical identification for oil pollution.<sup>166</sup> Baseline separation between saturated hydrocarbons (alkanes and cycloalkanes) and unsaturated hydrocarbons was achieved with the HPLC method and hydrocarbons with a boiling point from C<sub>8</sub> to C<sub>40</sub>, and better group-type separation and quantification was achieved compared to direct GC × GC.

## ■ ADSORPTION CHROMATOGRAPHY

Adsorption chromatography, or column chromatography, refers to separation of structural or functional groups from complex fluids in a glass column with a mobile phase. One of the most routinely applied methods for petroleum analysis is the SARA (saturates/aromatics/resins/asphaltenes) separation (ASTM D-2007), criticized due to its large solvent, adsorbent, and petroleum requirement. Several alternative methods were developed, and weight percent of each fraction recovered compared for two different crude oils and are shown to vary widely between published alternative SARA methods.<sup>167</sup> Open-column liquid chromatography or preparative liquid chromatography has been applied to the characterization of heavy hydrocarbons extensively in the past decades. Separations on adsorbents, such as silica gel or alumina, are based on well-known retention and elution mechanisms, and polarity differences between the adsorbent and sample govern the sample

retention process. With appropriate adsorbent and solvent (or solvent mixtures), components that differ in polarity are displaced inversely with polarity, and successive elution with solvents with higher polarity solvents elute components retained on the adsorbent low-polarity eluants.<sup>116</sup>

**Asphalten Fractionation.** Routine on-column fractionation methods for asphaltenes suffer from irreversible adsorption due to the high polarity of asphaltenes. Boduszynski et al. developed a chemical method of separation based on reactivity that utilized anion and cation resins to separate components of heavy crude oil and asphaltenes capable of hydrogen bonding, followed by coordination chemistry on clay and obtained a neutral Lewis base and hydrocarbon fraction, which was further separated on silica gel into saturated and aromatic hydrocarbons.<sup>168</sup> Although SARA separations require an initial asphaltene precipitation, the maltene fraction is further separated into saturate, aromatic, and resin fractions; however, there is no routine method for subfractionation of asphaltenes. Schabron et al. developed an on-column precipitation and redissolution separation technique for asphaltenes and heavy petroleum fractions on an inert stationary phase (polytetrafluoroethylene, PTFE) that is strictly solubility-based.<sup>169</sup> Asphaltenes are loaded on a PTFE-packed column and precipitated from crude oil with heptane and can be either redissolved in a single strong solvent or in three sequential steps with solvents of increasing solvent strength at different temperatures. The application of the asphaltene determinator method extends to both up- and downstream samples, such as whole crude oils, fuel oils, and atmospheric and vacuum residue.

## ■ SOLUBILITY PARAMETER

The solubility parameter describes the interaction between molecules in a condensed phase and is applied to petroleum to predict solubility and affinity between heavy crude components and their surroundings, important especially for reservoir conditions. Often, pressure–volume–temperature properties required for conventional solubility parameter calculations for live crude at reservoir conditions are unavailable. Zhang and co-workers developed a simple equation that relates solubility parameters to measured density by a linear function for live reservoir fluids at elevated temperature and pressures.<sup>170</sup> Combined with the Peng–Robinson equation of state, solubility parameters were calculated for four pure hydrocarbons and dead and live oils at elevated pressure (0.1–150.7 MPa) and reservoir temperature (323.9–422.0 K). Solubility parameters of live reservoir fluids were related to their measured densities by a linear function for 45 reservoir fluids and predicted solubility parameters correlated with previously published methods. Acevedo et al. applied the Sphere method to calculate components of solubility parameters (dispersion, polar, and hydrogen bonding) and applied the method to resins, asphaltenes, and two asphaltene fractions.<sup>171</sup> The authors report solubility behavior for all samples and a method to predict solubility behavior based on calculated solubility parameters and predict high affinity between asphaltenes and resins and suggest that resins increase the solubility of asphaltenes in good solvents, a departure from the long-standing Nellensteyn model.

## ■ NUCLEAR MAGNETIC RESONANCE

Nuclear magnetic resonance (NMR) has been frequently used for general studies of the composition and structural analysis of petroleum fractions. NMR directly measures aromatic and aliphatic carbon (<sup>13</sup>C) and hydrogen distributions (<sup>1</sup>H) and

provides important information on the carbon and hydrogen structural groupings in a molecule.<sup>13</sup>C NMR evaluations of coal and asphaltenes pioneered early NMR applications for petroleum analysis.<sup>172,173</sup>

An important study applied solid-state <sup>13</sup>C NMR to characterize the structure and average chemical composition of carbon presented in kerogen from different types of organic matter and degree of maturity, and X-ray photoelectron spectroscopy (XPS) agreed with <sup>13</sup>C NMR quantitation of aromatic carbon.<sup>174</sup> The direct characterization of nitrogen, sulfur, and oxygen chemical moieties in kerogens from different organic matter provides fundamental information necessary for structural models. Although the total amount of organic nitrogen and sulfur varies across studied kerogens, the patterns observed in oxygen, nitrogen, and sulfur speciation are consistent. Singly bound C—O species and carbonyl—carboxyl species decrease with increased aromatic carbon, whereas aromatic sulfur species increase with a higher amount of aromatic carbon. However, the majority of nitrogen species are pyrrolic for all kerogen types. Kelemen et al. recently applied <sup>13</sup>C NMR and sulfur X-ray absorption near edge structure spectroscopy (S-XANES) and XPS to characterize solid bitumen samples which form problematic insoluble organic residues through thermochemical sulfate reduction (TSR) or thermal chemical alteration (TCA) through reservoir processes associated with petroleum migration.<sup>175</sup> Difficulty arises in differentiation between bitumen formed by TSR or TCA, since both occur under relatively high temperatures, but compositional differences vary widely based on oxidative processes and therefore, the ability to differentiate between TSR-TCA-derived bitumen is critical for efficient production strategies. TSR-solid bitumen is highly aromatic, sulfur-rich with low amounts of nitrogen, whereas TCA-solid bitumen is derived from polar materials initially rich in sulfur and nitrogen. Importantly, observed changes in abundance and speciation of organic nitrogen and sulfur were a function of thermal maturation and can consequently direct development of average structural models that can be coupled with known reaction pathways to predict thermal conversion to products in laboratory/geologic conditions.

Yang and Hirasaki presented a novel method for NMR measurement and raw data interpretation to correct for the  $T_2$  relaxation times commonly problematic for NMR logging of heavy crude oil and bitumen.<sup>176</sup> Here, the authors address common limitations associated with NMR measurements of highly viscous crudes through application of Curie's Law. A recent study that combined <sup>1</sup>H NMR with mass spectroscopy has been applied to determine wax precipitation temperatures for quantification and agreed with DSC results.<sup>177</sup> Wax samples precipitated from crude oil at different temperatures were analyzed to detect crude oil entrained in wax deposits based on <sup>1</sup>H NMR measurements, and results suggest a decrease in crude oil entrainment at lower precipitation temperatures.

## NMR FOR ASPHALTENE CHARACTERIZATION

NMR diffusion measurements on solid crude oil fractions (deposits and asphaltenes) provide vital information on molecular size, distributions, and interactive dynamics between molecules. Direct detection and identification of NMR signal from asphaltene molecules directly is difficult due to short relaxation times and weak signal, but the presence of asphaltenes greatly affects the relaxation properties of other molecules in petroleum samples. Therefore, asphaltene properties can be indirectly determined.

**Aggregation.** Low-field <sup>1</sup>H NMR has been reported as a quantitative method to determine asphaltene aggregation, since proton Larmor frequencies of a few megahertz are ideal for correlation times at hundreds of megahertz, well-suited for aggregated asphaltene clusters.<sup>178</sup> Lisitza et al. compare and discuss two NMR techniques commonly used to determine asphaltene aggregation.<sup>179</sup> Here, two techniques which directly detect molecular sizes and dynamics are discussed: spin-echo data, based on rotations and internal motion of asphaltene molecules, and translational diffusion data. A positive entropy of aggregation was reported and proposed to be a result of the presence of smaller molecules in the system which gain entropy when larger molecules form aggregates. A new theoretical method, the porous asphaltene model, attributes the ability of an asphaltene aggregate to serve as a relaxing agent to other species of its size through comparison of longitudinal and transverse relaxation rates, and results correlated with small-angle X-ray scattering. Because of the lack of aromatic protons in asphaltene fractions, several new NMR methods have been recently introduced. Durand et al. applied <sup>1</sup>H diffused-ordered spectroscopy (DOSY) nuclear magnetic resonance based on pulsed field gradient (PFG) sequences to obtain physical and chemical information on hydrocarbon mixtures and asphaltenes.<sup>180</sup> However, because asphaltene molecule exhibit a concentration and solvent-based tendency to self-associate, a bidimensional sequence of the DOSY sequence was not observed with conventional pulsed-field-gradient spin echo (PFGSE) DOSY NMR experiments.<sup>181</sup> Low-field NMR with two-dimensional diffusion-relaxation distributions have been developed to increase information on chemical composition for a series of hydrocarbon mixtures and determined that asphaltene content could be used to characterize the process of asphaltene aggregation in crude oil.<sup>182</sup>

**Structure.** Multiplet selective NMR techniques have been used to characterize the degree of condensation and alkyl substitution on aromatic rings in asphaltenes of different origin and determined that the average number of condensed aromatic rings in most asphaltenes is seven.<sup>183</sup> Earlier studies by Murphy and co-workers applied <sup>13</sup>C and <sup>1</sup>H dipolar dephasing NMR experiments to asphaltenes from coal liquids and determined the structure to be primarily composed of polycyclic condensed rings with a condensation index of 3 or less, with large variations in aliphatic side chain length and branching.<sup>184</sup> A recent concentration-based <sup>1</sup>H DOSY NMR study reported that asphaltenes from different origins contain both archipelago and continental-type structures and contain compounds which exhibit varying degrees of solubility in toluene.<sup>185</sup> Solid state <sup>13</sup>C single pulse magic angle spinning (MAS) and cross-polarization magic angle spinning (CP/MAS) have become standard high-resolution NMR methods for macromolecular characterization because it provides determination of aromaticity and abundance of each type of carbon atom. However, spinning side bands, long acquisition time, and incomplete magnetization transfer can compromise band assignments if magic angle spinning is not sufficiently high. A study on multi-sequence MAS/NMR experiments was recently conducted on a field deposit from the Hassi-Messaoud oil field in Algeria to gain improve signal efficiency and increase the contribution from quaternary carbon atoms in the asphaltene fraction, and the single pulse experiment was concluded to be the most quantitative technique for aromaticity estimation.<sup>186</sup> However, the authors acknowledge that additional investigation is required to account for the contact time effect in several sequences.

## ■ FLUORESCENCE

The noncontact, nondestructive, quantitative analysis of crude oil throughout the entire production process, from reservoir to refinery, is highly desirable and lends itself to optical techniques. Fluorescence measurements of crude oil have been applied for more than 60 years to determine the presence of oil in drilling mud and core samples, since fluorescence is dominated by aromatic hydrocarbons and is a function of physical and chemical properties inherent to the crude. A complex absorption profile for most crude oils arises from the wide range of chemical and physical characteristics of crude oil.<sup>187</sup>

## ■ FLUORESCENCE SPECTROSCOPY: RESERVOIR CHARACTERIZATION

The fluorescence lifetime of crude oils is very sensitive to composition, heavy oils have shorter lifetimes than light crude, and the emission wavelength was shown to correlate to API gravity in the 1970s. A comprehensive review of fluorescence techniques used for the analysis of crude petroleum oils encompasses both industrial and research applications of optical techniques routinely applied to oil applications.<sup>187</sup> Techniques applied to bulk crudes, hydrocarbon-bearing fluid inclusions, and oil spills are highlighted. In addition, a separate review focuses solely on hydrocarbon fluid inclusion fluorescence, a powerful technique used to characterize valuable hydrocarbon fluids trapped in geological fluid inclusions.<sup>188</sup> Fluorescence lifetime microscopy is a powerful, nondestructive technique for inclusion and reservoir characterization that differentiates trapped oils from different sources or charges. Lifetime differences between heavy and light crude oils can be used to differentiate between the chemical compositions of entrapped oil based on *in situ* measurements of different inclusions.<sup>189</sup>

Downhole fluid analysis (DFA) utilizes spectroscopy *in situ* to assess reservoir compartmentalization and hydrocarbon compositional grading critical for efficient production strategies. Two major production issues have been extensively characterized by fluorescence techniques: asphaltenes, which aggregate and flocculate out of the crude and cause deposition, and water-in-oil emulsions. Andrews et al. applied downhole fluorescence measurements to monitor subsurface heavy oil emulsions and reported fluorescence intensities independent of emulsion formation but dependent on the heavy oil alone and provided an effective method to determine variations in heavy oil type in oil columns in subsurface reservoirs.<sup>190</sup>

**Optical Spectroscopy.** Ruiz-Morales and Mullins further investigated previous results and reported the absorption and emission spectra of asphaltenes based on optical absorption and fluorescence emission and molecular orbital calculations to create a range of possible asphaltene molecular structures and report a probable asphaltene structure composed of seven fused rings per molecule.<sup>191</sup> In addition, the optical spectroscopy of crude oils and asphaltenes in the triplet excited state was recently reported based on femtosecond pump–probe spectroscopy and lifetimes also compared with molecular orbital calculations and concluded the predominant chromophore in asphaltenes and crude oils as five, six, and seven fused ring PAHs in further support of the island molecular architectural model.<sup>192</sup> Investigation of Langmuir films (surfactant molecules on surface of a liquid) for asphaltenes at the air–water interface based on several spectroscopic techniques showed the existence of nanoaggregates on the water surface that coexist with larger aggregates formed through compression<sup>193</sup> and further investigated

asphaltene characteristics at the interface in different solvents.<sup>194</sup> On the basis of *in situ* UV–vis spectroscopy at the air–water interface, the authors conclude the presence of toluene at longer times than previously thought and observe toluene trapped within asphaltene nanoaggregates. Importantly, this study emphasizes possible aromatic solvent trapping in asphaltene nanoaggregates, which could potentially produce erroneous results.

**Fluorescence Correlation Spectroscopy.** Fluorescence correlation spectroscopy (FCS) measures molecular diffusivities, and molecular size can be inferred without interference from aggregate formation. Therefore, FCS has been applied to characterize the translational diffusion of asphaltene molecules in dilute toluene, and the determined asphaltene molecular structure was dominated by a single aromatic core, in further support of the continental (island) model.<sup>195,196</sup>

**Time-Resolved Fluorescence.** Time-resolved fluorescence measurements have been employed for petroleum characterization, provide additional compositional information lost in time-averaging, steady-state methods, and elucidates the influence of quenching and energy transfer processes in crude oil, a complex mixture of fluorophores.<sup>187</sup> Time-resolved fluorescence depolarization (TRFD) has been applied to study asphaltene molecular size and structure in dilute solutions to characterize asphaltene monomers prior to aggregation, since depolarization rates are directly related to molecule size. A comparison with theoretical models and known chromophore standards coupled with rotational correlation times of individual asphaltene molecules derived a molecular weight range of 500–1000 amu with one or two aromatic chromophores per asphaltene molecule and sparked a lively debate in the literature about asphaltene molecular weight measurement techniques.<sup>197–199</sup> Correa and co-workers applied TRFD decay profiles to series of asphaltenes at different concentrations and reported persistent aggregation at concentrations as low as 0.8 g/L below the reported CNAC. The authors introduced a distribution analysis method based on the linear relationship between long and short lifetime components of time-resolved decay profiles and conclude asphaltene structure as polyaromatic rings with four or more rings per monomer.<sup>200</sup>

## ■ CENTRIFUGE AND ULTRAFILTRATION

Shaw and co-workers first acknowledge the failure to account for solid maltenes in rheological methods, which can lead to erroneous viscosity measurements for asphaltenes. The authors included viscosity impacts from nonasphaltenic solids (maltenes) and first pointed out the importance of their role in viscosity determination for permeates, retentates, and feeds associated with heavy crude and bitumen.<sup>201</sup> A study on the mass fraction of resins in asphaltene-rich nanoaggregates applies a mass balance model and data regression fits to SARA fractions of permeate and retentate samples through solvent-free direct filtration through 5–200 nm filters and explores the contributions of resins locked in asphaltene aggregates and discuss limitations to modeling and analytic approaches for asphaltene characterization.<sup>202</sup>

Centrifugation at elevated temperatures was applied to create a large, equilibrium asphaltene gradient to mimic reservoir conditions and concluded that the maximum and minimum asphaltene aggregation number ranged between 3 and 8 monomers per aggregate, in support of the modified Yen model.<sup>203</sup> A centrifugation study of asphaltenes near the critical nanoaggregate concentration (CNAC) determines nanoaggregates size ~2.5 nm based

on gravitational gradients and discusses limitations on the commonly used two-component (monomer and nanoaggregates), phase equilibrium model.<sup>204</sup> A study conducted in 2010 first demonstrated that crude oils can pass through 30 nm Gore-Tex membranes without alteration of asphaltene content or transport properties and provided a method for small volume membrane separation to isolate pure, representative crude oil samples with negligible asphaltene loss and removal of water from emulsions.<sup>205</sup>

## ■ HIGH-Q ULTRASONIC SPECTROSCOPY

One of the most fundamental properties that must be acknowledged in studies of asphaltenes is their tendency to self-associate in a hierarchy: monomers self-associate at the molecular level and form aggregates and aggregate self-association leads to flocculation, which causes deposition throughout all stages of petroleum production. The polydispersity of molecular composition associated with asphaltenes lends itself to perception of monomers as amphipathic, with both hydrophilic and hydrophobic moieties. Coupled with studies which attribute emulsion stability to asphaltenes at oil/water interfaces, asphaltene monomers have been often referred to as "surfactant-like". The micellar and colloidal models previously applied to describe the primary aggregation of asphaltenes in solution do not account for the polydispersity of asphaltene aggregates in solution. Sirota warned about the dangers of literal application of the colloidal analogy and attributed the temperature and concentration dependent viscosity of asphaltene mixtures to their proximity to the glass transition.<sup>206</sup> The asphaltene community began a departure from the colloidal-micellar model with the introduction of the "critical nanoaggregation concentration" (CNAC) by Mullins in 2005. On the basis of high-resolution ultrasonic spectroscopy, the authors reported the CNAC of asphaltenes in toluene at roughly 0.1 g/L with variability between asphaltenes from different crudes.<sup>207</sup> The discovery of self-association at orders of magnitude below previously reported critical micelle concentrations directed asphaltene researchers away from concentrations where asphaltenes were already aggregated and led to more accurate and scientifically sound conclusions about asphaltene aggregation. Since the introduction of the CNAC, several groups have reported observation of aggregates at concentrations below 0.1 g/L. Correa et al. reported asphaltene aggregates at 0.08 g/L based on time-resolved fluorescence decay profiles and attributed dimerization to  $\pi-\pi$  stacking between aromatic rings.<sup>208</sup>

## ■ X-RAY PHOTOELECTRON SPECTROSCOPY

Asphaltene deposition poses production, transport, and processing challenges and plagues the petroleum industry. Bitumen and heavy crude poses a significant challenge for efficient production due to the inherent high asphaltene content. Several groups have been studying asphaltene deposition based on XPS to observe functional groups on asphaltene deposit surfaces. Shaw and co-workers analyzed bitumen residues on acidic and basic substrates by X-ray photoelectron spectroscopy.<sup>208</sup> Thicker deposits observed on acidic substrates had a lower sulfur content than the parent residue while thinner deposits observed on basic substrates were enriched in sulfur relative to the residue. This important observation is noteworthy because asphaltenes are known to have high sulfur content, but the lower sulfur content species in residue are more strongly sorbed on acidic substrates than higher sulfur content species and less quickly on basic/neutral substrates. Sjöblom and co-workers investigated

asphaltene surface properties and aggregation based on water plasma modification to the polar nature of asphaltenes followed by XPS measurements.<sup>209</sup> On the basis of XPS measurements, the authors observed significant oxygen percentage increases from 1.5 to 12 that correlated to water plasma exposure time, although sulfur and nitrogen remained relatively constant. A gradual change in asphaltene properties up to 10 min, followed by a breaking point at extended treatment times, was attributed to changes in asphaltene structure and plasma composition over time. Experimental results were fitted to a dose-response model, which was used to correlate plasma chemical modification to solubility, and longer exposure times led to higher levels of asphaltenes of low solubility. The authors observed a change in contact angle and adsorption properties at longer plasma treatment times and postulated fragmentation of alkyl chains that release oxidized species into the plasma.

## ■ SMALL ANGLE X-RAY SCATTERING

Small angle scattering techniques have been applied extensively to characterize asphaltenes, and Sheu presented a detailed review on scattering for structural characterization of asphaltene aggregates.<sup>210</sup> Small angle X-ray scattering (SAXS) makes use of the electron density differences to identify and measure the particle size, shape, and polydispersity on the colloidal scale. Differences in electron densities between asphaltene aggregates and their surrounding solvent or hydrocarbon matrix can be used to detect asphaltene aggregates in crude oils.<sup>210</sup> Barre et al. applied SAXS measurements as a function of concentration to probe the fractal description of asphaltene aggregates after ultracentrifugation, and results support a hard sphere model to predict the viscosity of solutions from structural measurements.<sup>211</sup>

## ■ SMALL ANGLE NEUTRON SCATTERING

Small angle neutron scattering (SANS) applies a similar principle to SAXS except the contrast required for detection of an object from its surroundings is the scattering length density, dependent on the difference of the nuclei within the molecules.<sup>210</sup> Neutron scattering cross section between asphaltene molecules and surrounding molecules requires dissolution of asphaltene in deuterated solvents to enhance contrast for SANS, since asphaltenes do not generally have enough contrast for neutrons to distinguish them from their surroundings.<sup>210</sup> A combination of SANS and SAXS measurements on asphaltenes by Sirota in 2004 challenged the asphaltene colloidal aggregate model and attributed scattering to any one-phase liquid mixture of unlike molecules, thereby further improving the role of asphaltenes in phase behavior, morphology, and viscosity.<sup>206</sup>

An important study by the Kilpatrick group highlighted the importance of inclusion of solvation effects within asphaltene aggregates in SANS measurements, which can lead to erroneous molecular weight and size calculations.<sup>212</sup> The same group further studied asphaltenes dissolved in binary solvent mixtures and observed preferential solvent entrainment within asphaltene aggregates.<sup>213</sup> SANS and V-SANS measurements report aggregate sizes for asphaltene aggregates redispersed in deuterated toluene similar to aggregate size measurements on whole crude oils and suggest two different aggregate size distributions that coexist.<sup>214</sup>

Although neutron reflectivity is lauded as a powerful technique for characterization interfaces, the strong neutron absorption at liquid–liquid interfaces requires an increase in the area-to-volume conditions to use SANS techniques. Interfacial layers

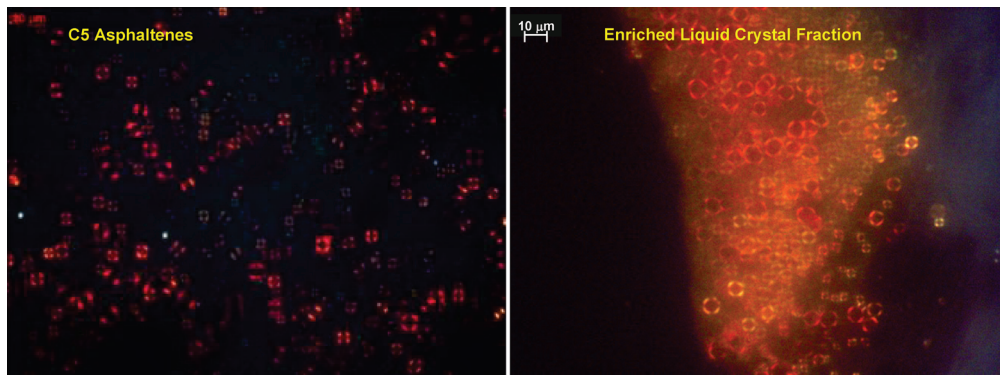


**Figure 3.** Polarized light microscopy images of asphaltene liquid crystalline state. Here, C<sub>5</sub> asphaltenes (left) are compared with an enriched liquid crystal sample (right). The C<sub>5</sub> asphaltenes have the lowest amount of liquid crystals, which are small ( $10\text{ }\mu\text{m}$ ) and spread out. For the enriched samples, a higher amount of liquid crystals were observed. The authors graciously thank Professor John M. Shaw and Brady Masik from the University of Alberta for providing the liquid crystal images.

formed by asphaltenes at the oil–water interface were studied directly by SANS to determine the interfacial layer thickness and asphaltene aggregate size, and results correlated to the surface rheology and emulsion stability measurements.<sup>215</sup> SANS measurements were modeled with a polydisperse core/shell form factor and thin sheet approximation to study the film thickness and asphaltene composition from model emulsion systems and present the first method to characterize emulsion film composition *in situ* for emulsion stability.<sup>216</sup> A separate study by Alvarez et al. combined SANS and UV–vis spectrometry to measure the interfacial thickness between crude oil and water in emulsions stabilized by asphaltenes and concluded a relationship between aggregate size and interfacial thickness.<sup>215</sup> Because emulsion breakage on free water molecules is easier than after water absorbs onto polar sites on asphaltenes at the interface, the importance of understanding the behavior of water molecules in emulsions upon storage is critical. Sheu and co-workers reported that water molecules in a petroleum emulsion transform from a free state to a restricted/bound state during storage based on the free energy of the emulsion system based on calorimetry and inelastic neutron scattering measurements.<sup>217</sup> Upon storage, the majority of the water molecules in the emulsion are free but after a week of storage, ~90% of the water molecules had phase separated. The authors show that water molecules resemble bulk ice as free water molecules in water-in-oil emulsion before separation to the bottom phase after 5–7 days of storage.

## ■ ADVANCES IN ASPHALTENE CHARACTERIZATION

**Direct-Current (dc) Electrical Conductivity.** Zeng et al. applied direct-current (dc) electrical conductivity as a function of asphaltene concentration to extrapolate the critical nanoaggregate concentration (CNAC) for petroleum asphaltenes and compare the conductivity above and below the CNAC and report the aggregation number less than 10 in agreement with previously reported alternating-current conductivity and high-Q ultrasonic measurements.<sup>218</sup> The role of resins on asphaltene stability has been controversial, and several conflicting views can be found in the literature. A recent study by Sedghi and Goual challenged the Nellensteyn hypothetical model, where resins adsorb on asphaltenes and provide a steric, stabilizing layer for asphaltene aggregates.<sup>219</sup> Here, the authors present results which challenge the Nellensteyn model based on impedance analysis. Observed

variations by charge carriers in petroleum that act as tracers for dc conductivity measurements does not support resins as a stabilizing layer for asphaltene aggregates. Direct current conductivity measurements at a low concentration of asphaltenes in toluene and heptane/toluene mixtures conclude that a low number (less than 10) of asphaltene nanoaggregates at a low concentration in toluene with a low amount of resins. Therefore, this study shows that asphaltenes are not sterically stabilized by resins at the concentration range investigated. Only in heptane/toluene mixtures were the least soluble resins shown to enhance asphaltene stability, since they tend to aggregate with asphaltenes. This result is in support of a thermodynamic model for asphaltene–resin aggregate formation proposed by Rogel in 2008.<sup>220</sup>

**Liquid Crystal Asphaltenes.** The observation of liquid crystals in asphaltenes precipitated from petroleum solids from different geological origin was first observed and reported by the Shaw group, and the authors concluded that liquid-crystal domains arise from multiple thermal and solvent addition pathways, which may facilitate development of structure-based separation methods for heavy crude components.<sup>221</sup> This monumental observation of amphotrophic liquid crystals and specific attributes of the liquid-crystal structure itself is the first reported occurrence of liquid crystals in nature. Understanding the role liquid crystals play in complex phase and interfacial behavior of petroleum provides an opportunity for development of petroleum partitioning methods. The liquid crystal domain was first observed in N<sub>2</sub> atmosphere at 330 K and disappeared at 430 K, and after subsequent cooling and reheating, the liquid-crystal domains did not reappear and the same observation was reported in the presence of toluene vapor at room temperature. Interestingly, the compositional diversity in petroleum and asphaltenes would be expected to prevent liquid crystal formation, since multiple components should interfere in liquid-crystal phase formation. However, precipitated asphaltenes are solid, and therefore, the authors postulated the presence of liquid crystal domains previously not observed in whole petroleum since smaller components would act as solvents and disrupt formation. On the basis of microscopic observations, three phases for asphaltenes were observed between 350 and 430 K: solid, liquid-crystal, and isotropic liquid. The liquid crystal domain for all examined samples exhibited a ring of liquid crystal around a solid core, possibly due to the precipitation mechanism (see Figure 3). Multiple thermal and solvation pathways for liquid crystal formation in petroleum

fractions were observed, and dissolution in strong solvents/petroleum liquids at higher temperature disrupts crystalline order or formation. Phase behavior predictions for asphaltene deposition in production/refining previously did not account for liquid-crystal domain formation, and results presented in this work could account for inaccuracies in deposition prediction.

## ■ PETROLEOMICS

As highlighted above, the advances in analytical technology and molecular level compositional/structural information are ideal for petroleomic applications, where compositional information predicts behavior and reactivity for compositional comparison of crudes. Klein et al. have addressed the kinetic modeling of a range of different processes, catalytic reforming, lignin thermolysis, and resid.<sup>222–224</sup> Ultimately, models determine the required level of information. Therefore, data from most advanced methods need to be incorporated into the models to determine the level of compositional information required to accurately model feed X in refinery process Y.

Ventura and co-workers demonstrated the use of GC × GC for compound class fingerprinting to determine the similarity of down hole collected oil samples.<sup>225</sup> The authors use spider diagrams to visualize the complex data sets and conclude that although useful for source and thermal history of oils, biomarkers are not always reliable for oil similarity comparisons. The work expands the number of compounds classes that may be employed to assess oil similarity. In a noteworthy demonstration of the power of state of the art comprehensive 2-D GC, Ventura et al. recently updated the approach through the addition of multiway principal components analysis (MPCA) to determine oil similarity. They demonstrate the utility of MPCA (~3500 quantified components) to resolve multimolecular differences between oil samples and provide insight into the global molecular relatedness between crude oils.<sup>226</sup> Nouvelle and Coutrot address similar issues (connectivity/compartmentalization/oil similarity) with a Malcolm distribution method for GC fingerprinting of crude oils.<sup>227</sup> The statistical method, based on a consistent quantification of the uncertainty in peak height measurements, allows for the determination of absolute distances between GC fingerprints on a universal scale. Fernández-Varela and co-workers evaluated the effectiveness of three unsupervised pattern recognition techniques to group oils by geographic origin on a 34 sample set of crude oils that relied on 28 diagnostic ratios determined by GC/MS.<sup>228</sup>

In a noteworthy pair of manuscripts, Arey et al. systematically addressed compositional changes in weathered petroleum samples in an effort to reveal the species that comprise the “unresolved complex mixture” by GC × GC analysis.<sup>140</sup> They mapped hydrocarbon vapor pressure and aqueous solubility and projected it onto the compositional space accessible by comprehensive 2-D GC analysis of 13 weathered oil samples. The authors report methods to quantitatively decouple mass loss patterns associated with evaporation and water washing. In part 2 of this series, they expand on the approach with the inclusion of a mass transfer model to address the patterns of species lost by water washing (dissolution) and evaporation identified in Part 1 of the 2-part series.<sup>141</sup> The model successfully predicted the GC × GC chromatogram patterns of the mass removal associated with evaporation, water-washing, and diffusion limited transport. Chen et al. predicted molecular weight vs boiling point distribution curves of middle distillates by GC-FIMS.<sup>229</sup> The authors address the determination of the response factor for compound types, data management, and MW prediction for 12 distillate cuts that span a

wide range of hydrocarbon types and note that the technique predicted the molecular weight versus boiling point curves with an average deviation of 3.2%. Ha and co-workers address the union of PONA (paraffin, isoparaffin, olefin, naphthalene, and aromatics), a method useful for species that boil below 200–360 °C, data for a detailed, quantitative hydrocarbon type analysis across the entire middle distillate range.<sup>230</sup> Data reconciliation between PONA and GC-FIMS is described in detail, and the authors present the comparisons of conventional SimDis and the newly developed FIMS-generated Sim-Dis results that are incredibly similar.

Hur et al. have tackled the inevitable task of combining statistical methods to complex FT-ICR MS data sets for a more comprehensive molecular level interpretation of the petroleome.<sup>231</sup> The analysis of 40 petroleum FT-ICR mass spectra by principal components analysis (PCA) and hierarchical cluster analysis (HCA) grouped the samples by molecular composition (PCA) that facilitated the visualization of compositional differences between sample and compositional similarity (HCA) based on a subset of selected peaks. Ahmed and co-workers applied the Mason–Schamp equation and IM-MS to identify structurally related compounds in crude oil.<sup>232</sup> Grossly separated in boiling point with an atmospheric-pressure solids analysis probe (ASAP) and subsequently analyzed by IM-MS, petroleum species that share similar structural cores align while differences in aromaticity led to nonlinear results. Thus, an increase in alkylation from a single core yielded a linear correlation and growth in the aromatic core (from 1 to 2 aromatic rings) resulted in unaligned data points, consistent with a discontinuous increase in collision cross section with increased mass.

## ■ AUTHOR INFORMATION

### Corresponding Author

\*E-mail: rodgers@magnet.fsu.edu.

## ■ BIOGRAPHIES

**Ryan P. Rodgers**, PhD., is a Scholar-Scientist and Director of the Environmental, Forensic and Petroleum Applications in the Ion Cyclotron Resonance program at the National High Magnetic Field Laboratory at Florida State University in Tallahassee, Florida. He received his Bachelor of Science in Chemistry from the University of Florida in 1995 and his Doctor of Philosophy in Analytical Chemistry from Florida State University in 1999. He is the co-founder of the field of “Petroleomics” and established the Petroleum, Environmental and Forensics Applications group at NHMFL in 2001. Results from past collaborations aided in the establishment of 7 FT-ICR MS facilities in academic and industrial oil research laboratories in the past 10 years.

**Amy M. McKenna**, PhD., is an Assistant Scholar-Scientist and directs the Ion Cyclotron Resonance external user program at the National High Magnetic Field Laboratory. The facility serves more than 100 external users each year, with research from petroleum and environmental applications. She received her Bachelor of Science from the University of Tampa in 2005 and her Doctor of Philosophy in Analytical Chemistry from Florida State University in 2009. Her research focuses on heavy oil and asphaltene characterization.

## ■ ACKNOWLEDGMENT

The authors thank Christopher M. Reddy, Robert K. Nelson, and Karin Lemkau from the Department of Marine Chemistry

and Geochemistry at Woods Hole Oceanographic Institute. The authors would like to acknowledge the National High Magnetic Field Laboratory, funded by the National Science Foundation Division of Materials Research (Grant DMR-06-54118), Florida State University, and the State of Florida. The author kindly thank Professor John M. Shaw and Brady Masik of the University of Alberta, Department of Chemical and Materials Engineering for their assistance.

## NOMENCLATURE

ESI	electrospray ionization	DBE	double bond equivalents (number of rings + double bonds)
MS	mass spectrometry	TLC	thin layer chromatography
FT-ICR MS	Fourier transform ion cyclotron resonance mass spectrometry	OES	optical emission spectroscopy
EASI	easy ambient sonic-spray ionization	SEC	size exclusion chromatography
DESI	desorption electrospray ionization	MIC	microwave induced combustion
DART	direct analysis in real time	TAN	total acid number
FI	field ionization	OSPW	oil sands production water
PAH	polycyclic aromatic hydrocarbon	HTGC	high-temperature gas chromatography
AP	atmospheric pressure	DFA	down-hole fluid analysis
LIAD	laser induced acoustic desorption	OM	organic matter
CI	chemical ionization	OSDC	organic solids deposition control
EI	electron ionization	IRMS	isotope ratio mass spectrometry
APPI	atmospheric pressure photo-ionization	BP	before present
APCI	atmospheric pressure chemical ionization	Py	pyrolysis
LD	laser desorption	WAT	wax appearance temperature
LI	laser ionization	DSC	differential scanning calorimetry
LDI	laser desorption/ionization	WPC	wax precipitation curve
L <sup>2</sup> MS	two step laser mass spectrometry	SPE	solid phase extraction
UV	ultraviolet	ADC	advanced distillation curve
IR	infrared	MDGC	multidimensional gas chromatography
VUV	vacuum ultraviolet	NCD	nitrogen chemiluminescence detector
PIMS	photo-ionization MS	SCD	sulfur chemiluminescence detector
He	helium	SFE	supercritical extraction
GC	gas chromatography	RICO	ruthenium ion catalyzed oxidation
GC/MS	gas chromatography/mass spectrometry	DAD	diode array detector
Ni	nickel	THF	tetrahydrofuran
MALDI	matrix assisted laser desorption ionization	CE	capillary electrophoresis
FD	field desorption	HDS	hydrodesulfurization
TOF and TOF-MS	time-of-flight mass spectrometry	XPS	X-ray photoelectron spectroscopy
PSD	post source decay	S-XANES	sulfur X-ray absorption near edge structure
GPC	gel-permeation chromatography	PFG	pulsed field gradient
HPLC	high-performance liquid chromatography	MAS	magic angle spinning
LIFDI	liquid injection field desorption/ionization	FCS	fluorescence correlation spectroscopy
ICP	inductively coupled plasma	TRFD	time-resolved fluorescence
PFM	produced formation water	CNAC	depolarization
LC	liquid chromatography	SAXS	critical nanoaggregate concentration
GC × GC	comprehensive gas chromatography	SANS	small angle X-ray scattering
FID	flame ionization detector	DC	small angle neutron scattering
IM-MS	ion mobility-mass spectrometry		direct current
SARA	saturates, aromatics, resins, and asphaltenes		
HVGQ	heavy vacuum gas oil		
DMO	de-metalized oil		
VGO	vacuum gas oil		
NPD	nitrogen phosphorus detector		
AED	atomic emission detector		
NMR	nuclear magnetic resonance		

## REFERENCES

- (1) Zhan, D.; Fenn, J. B. *Int. J. Mass Spectrom.* **2000**, *194*, 197–208.
- (2) Qian, K.; Rodgers, R. P.; Hendrickson, C. L.; Emmett, M. R.; Marshall, A. G. *Energy Fuels* **2001**, *15*, 492–498.
- (3) Qian, K.; Robbins, W. K.; Hughey, C. A.; Cooper, H. J.; Rodgers, R. P.; Marshall, A. G. *Energy Fuels* **2001**, *15*, 1505–1511.
- (4) Quann, R. J.; Jaffe, S. B. *Ind. Eng. Chem. Res.* **1992**, *31*, 2483–2497.
- (5) Corilo, Y. E.; Vaz, B. G.; Simas, R. C.; Nascimento, H. D. L.; Klitzke, C. F.; Pereira, R. C. L.; Bastos, W. L.; Neto, E. V.; Rodgers, R. P.; Eberlin, M. N. *Anal. Chem.* **2010**, *82*, 3990–3996.
- (6) Alberici, R. M.; Simas, R. C.; de Souza, V.; de Sa, G. F.; Daroda, R. J.; Eberlin, M. N. *Anal. Chim. Acta* **2010**, *659*, 15–22.
- (7) Wu, C.; Qian, K.; Neffli, M.; Cooks, R. G. *J. Am. Soc. Mass Spectrom.* **2010**, *21*, 261–267.
- (8) Rummel, J. L.; McKenna, A. M.; Marshall, A. G.; Eyler, J. R.; Powell, D. H. *Rapid Commun. Mass Spectrom.* **2010**, *24*, 784–790.
- (9) Crawford, K. E.; Campbell, J. L.; Fiddler, M. N.; Duan, P.; Qian, K.; Gorbaty, M. L.; Kenttamaa, H. I. *Anal. Chem.* **2005**, *77*, 7916–7923.

- (10) Nyadong, L.; McKenna, A. M.; Hendrickson, C. L.; Rodgers, R. P.; Marshall, A. G. *Anal. Chem.* **2011**, *83*, 1616–1623.
- (11) Gao, J.; Borton, D. J., II; Owen, B. C.; Jin, Z.; Hurt, M.; Amundson, L. M.; Madden, J. T.; Qian, K.; Kenttamaa, H. I. *J. Am. Soc. Mass Spectrom.* **2011**, *22*, 531–538.
- (12) Purcell, J. M.; Hendrickson, C. L.; Rodgers, R. P.; Marshall, A. G. *Anal. Chem.* **2006**, *78*, 5906–5912.
- (13) Haapala, M.; Purcell, J. M.; Saarela, V.; Fransila, S.; Rodgers, R. P.; Hendrickson, C. L.; Kotiaho, T.; Marshall, A. G.; Kostiainen, R. *Anal. Chem.* **2009**, *81*, 2799–2803.
- (14) Kim, S.; Rodgers, R. P.; Blakney, G. T.; Hendrickson, C. L.; Marshall, A. G. *J. Am. Soc. Mass Spectrom.* **2009**, *20*, 263–268.
- (15) Kim, Y. H.; Kim, S. *J. Am. Soc. Mass Spectrom.* **2010**, *21*, 386–392.
- (16) Schmitt-Kopplin, P.; Englmann, M.; Rosella-Mora, R.; Schiewek, R.; Brockmaan, K. J.; Benter, T.; Schmitz, O. J. *Anal. Bioanal. Chem.* **2008**, *391*, 2803–2809.
- (17) Pomerantz, A. E.; Hammond, M. R.; Morrow, A. L.; Mullins, O. C.; Zare, R. N. *J. Am. Chem. Soc.* **2008**, *130*, 7216–7217.
- (18) Hortal, A. R.; Martinez-Haya, B.; Lobato, M. D.; Pedrosa, J. M.; Lago, S. *J. Mass Spectrom.* **2006**, *41*, 960–968.
- (19) Tanaka, R.; Sato, S.; Takanohashi, T.; Hunt, J. E.; Winans, R. E. *Energy Fuels* **2004**, *18*, 1405–1413.
- (20) Apicella, B.; Alfe, M.; Amoresano, A.; Galano, E.; Ciajolo, A. *Int. J. Mass Spectrom.* **2010**, *295*, 98–102.
- (21) Pomerantz, A. E.; Hammond, M. R.; Morrow, A. L.; Mullins, O. C.; Zare, R. N. *Energy Fuels* **2009**, *23*, 1162–1168.
- (22) Hurtado, P.; Gamez, F.; Martinez-Haya, B. *Energy Fuels* **2010**, *24*, 6067–6073.
- (23) Sabbah, H.; Morrow, A. L.; Pomerantz, A. E.; Mullins, O. C.; Tan, X.; Gray, M. R.; Azyat, K.; Tykwienski, R. R.; Zare, R. N. *Energy Fuels* **2010**, *24*, 3589–3594.
- (24) Guo, W.; Bi, Y.; Guo, H.; Pan, Y.; Qi, F.; Deng, W.; Shan, H. *Rapid Commun. Mass Spectrom.* **2008**, *22*, 4025–4028.
- (25) Volk, H.; Fuentes, D.; Fuerbach, A.; Miese, C.; Koehler, W.; Baersch, N.; Barcikowski, S. *Org. Geochem.* **2010**, *41*, 74–77.
- (26) Siljestroem, S.; Hode, T.; Lausmaa, J.; Sjoevall, P.; Toporski, J.; Thiel, V. *Org. Geochem.* **2009**, *40*, 135–143.
- (27) Burgess, W. A.; Pittman, J. J.; Marcus, R. K.; Thies, M. C. *Energy Fuels* **2010**, *24*, 4301–4311.
- (28) Flego, C.; Zannoni, C. *Energy Fuels* **2010**, *24*, 6041–6053.
- (29) Smith, D. F.; Schaub, T. M.; Rodgers, R. P.; Hendrickson, C. L.; Marshall, A. G. *Anal. Chem.* **2008**, *80*, 7379–7382.
- (30) Qian, K.; Edwards, K. E.; Siskin, M.; Olmstead, W. N.; Mennito, A. S.; Dechert, G. J.; Hoosain, N. E. *Energy Fuels* **2007**, *21*, 1042–1047.
- (31) Maryutina, T. A.; Soin, A. V. *Anal. Chem.* **2009**, *81*, 5896–5901.
- (32) Caumette, G.; Lienemann, C. P.; Merdrignac, I.; Paucot, H.; Bouyssiere, B.; Lobinski, R. *Talanta* **2009**, *80*, 1039–1043.
- (33) Ricard, E.; Pechevran, C.; Sanabria Ortega, G.; Prinzhofner, A.; Donard, O. F. X. *Anal. Bioanal. Chem.* **2011**, *399*, 2153–2165.
- (34) Heilmann, J.; Boulyga, S. F.; Heumann, K. G. *J. Anal. At. Spectrom.* **2009**, *24*, 385–390.
- (35) Oliveira, E. P.; Yang, L.; Sturgeon, R. E.; Santelli, R. E.; Bezerra, M. A.; Willie, S. N.; Capilla, R. *J. Anal. At. Spectrom.* **2011**, *26*, 578–585.
- (36) Marshall, A. G.; Hendrickson, C. L. *Ann. Rev. Anal. Chem.* **2008**, *1*, 579–599.
- (37) Xian, F.; Hendrickson, C. L.; Blakney, G. T.; Beu, S. C.; Marshall, A. G. *Anal. Chem.* **2010**, *82*, 8807–8812.
- (38) Savory, J. T.; Kaiser, N. K.; McKenna, A. M.; Xian, F.; Blakney, G. T.; Rodgers, R. P.; Hendrickson, C. L.; Marshall, A. G. *Anal. Chem.* **2011**, *83*, 1732–1736.
- (39) Marshall, A. G.; Rodgers, R. P. *Proc. Nat. Acad. Sci. U.S.A.* **2008**, *105*, 18090–18095.
- (40) Phillips, J. P.; Xu, J. *J. Chromatogr., A* **1995**, *703*, 327–334.
- (41) McKenna, A. M.; Purcell, J. M.; Rodgers, R. P.; Marshall, A. G. *Energy Fuels* **2010**, *24*, 2929–2938.
- (42) McKenna, A. M.; Blakney, G. T.; Xian, F.; Glaser, P. B.; Rodgers, R. P.; Marshall, A. G. *Energy Fuels* **2010**, *24*, 2939–2946.
- (43) Becker, C.; Fernandez-Lima, F. A.; Russell, D. H. *Spectroscopy* **2009**, *24*, 38–42.
- (44) Fernandez-Lima, F. A.; Becker, C.; McKenna, A. M.; Rodgers, R. P.; Marshall, A. G.; Russell, D. H. *Anal. Chem.* **2009**, *81*, 9941–9947.
- (45) Strausz, O. P.; Morales-Izquierdo, A.; Kazmi, N.; Montgomery, D. S.; Payzant, J. D.; Safarik, I.; Murgich, J. *Energy Fuels* **2010**, *24*, 5053–5072.
- (46) Dutriez, T.; Courtiade, M.; Thiebaut, D.; Dulot, H.; Bertocini, F.; Hennion, M.-C. *J. Sep. Sci.* **2010**, *33*, 1787–1796.
- (47) Zhu, X.; Shi, Q.; Zhang, Y.; Pan, N.; Xu, C.; Chung, K. H.; Zhao, S. *Energy Fuels* **2011**, *25*, 281–287.
- (48) Al-Hajji, A. A.; Muller, H.; Koseoglu, O. R. *Oil Gas Sci. Techn.* **2008**, *63*, 115–128.
- (49) Li, N.; Ma, X.; Zha, Q.; Song, C. *Energy Fuels* **2010**, *24*, 5539–5547.
- (50) Wiwel, P.; Hinnemann, B.; Hidalgo-Vivas, A.; Zeuthen, P.; Petersen, B. O.; Duus, J. O. *Ind. Eng. Chem.* **2010**, *49*, 3184–3193.
- (51) von Muhlen, C.; de Oliveira, E. C.; Zini, C. A.; Caramao, E. B.; Marriott, P. J. *Energy Fuels* **2010**, *24*, 3572–3580.
- (52) Liu, P.; Xu, C.; Shi, Q.; Pan, N.; Zhang, Y.; Zhao, S.; Chung, K. H. *Anal. Chem.* **2010**, *82*, 6601–6606.
- (53) Liu, P.; Shi, Q.; Chung, K. H.; Zhang, Y.; Pan, N.; Zhao, S.; Xu, C. *Energy Fuels* **2010**, *24*, 5089–5096.
- (54) Jaspes, A.; Penassa, M.; Andersson, J. T. *Energy Fuels* **2009**, *23*, 2143–2148.
- (55) Mahe, L.; Dutriez, T.; Courtiade, M.; Thiebaut, D.; Dulot, H.; Bertocini, F. *J. Chromatogr., A* **2011**, *1218*, 534–544.
- (56) Kolbe, N.; van Rheinberg, O.; Andersson, J. T. *Energy Fuels* **2009**, *23*, 3024–3031.
- (57) Heilmann, J.; Heumann, K. G. *Anal. Chem.* **2008**, *80*, 1952–1961.
- (58) Heilmann, J.; Heumann, K. G. *Anal. Bioanal. Chem.* **2009**, *393*, 393–397.
- (59) Caumette, G.; Lienemann, C. P.; Merdrignac, I.; Bouyssiere, B.; Lobinski, R. *J. Anal. At. Spectrom.* **2009**, *24*, 263–276.
- (60) Soin, A. V.; Maryutina, T. A.; Arbuzova, T. V.; Spivakov, B. Y. *J. Anal. Chem.* **2010**, *65*, 571–576.
- (61) Mizanur Rahman, G. M.; Fahrenholz, T. M.; Kingston, H. M.; Pamuku, M.; Hwang, J. D.; Young, L. A. *Spectroscopy* **2010**, *25*, 36–45.
- (62) Tonietto, G. B.; Godoy, J. M.; Oliveira, E. P.; de Souza, M. V. *Anal. Bioanal. Chem.* **2010**, *397*, 1755–1761.
- (63) Pohl, P.; Vorapalawut, N.; Bouyssiere, B.; Carrier, H.; Lobinski, R. *J. Anal. At. Spectrom.* **2010**, *25*, 704–709.
- (64) Vorapalawut, N.; Pohl, P.; Bouyssiere, B.; Shiowatana, J.; Lobinski, R. *J. Anal. At. Spectrom.* **2011**, *26*, 618–622.
- (65) Xie, H.; Huang, K.; Liu, J.; Nie, X.; Fu, L. *Anal. Bioanal. Chem.* **2009**, *393*, 2075–2080.
- (66) Pereira, J. S. F.; Moraes, D. P.; Antes, F. G.; Diehl, L. O.; Santos, M. F.; Guimaraes, R. C.; Fonseca, T. C.; Dressler, V. L.; Flores, E. M. *Microchem. J.* **2010**, *96*, 4–11.
- (67) Caumette, G.; Dural, J.; Vorapalawut, N.; Merdrignac, I.; Lienemann, C. P.; Carrier, H.; Grassl, B.; Bouyssiere, B.; Lobinski, R. *J. Anal. At. Spectrom.* **2010**, *25*, 1123–1129.
- (68) Pohl, P.; Dural, J.; Vorapalawut, N.; Merdrignac, I.; Lienemann, C. P.; Carrier, H.; Grassl, B.; Bouyssiere, B.; Lobinski, R. *J. Anal. At. Spectrom.* **2010**, *25*, 1974–1977.
- (69) Qian, K.; Mennito, A. S.; Edwards, K. E.; Ferrugherelli, D. T. *Rapid Commun. Mass Spectrom.* **2008**, *22*, 2153–2160.
- (70) McKenna, A. M.; Purcell, J. M.; Rodgers, R. P.; Marshall, A. G. *Energy Fuels* **2009**, *23*, 2122–2128.
- (71) Qian, K.; Edwards, K. E.; Mennito, A. S.; Walters, C. C.; Kushnerick, J. D. *Anal. Chem.* **2010**, *82*, 413–419.
- (72) Dechaine, G. P.; Gray, M. R. *Energy Fuels* **2010**, *24*, 2795–2808.
- (73) Headley, J. V.; Peru, K. M.; Barrow, M. P. *Mass Spectrom. Rev.* **2009**, *28*, 121–134.
- (74) Smith, B. E.; Rowland, S. J. *Rapid Commun. Mass Spectrom.* **2008**, *22*, 3909–3927.

- (75) Fafet, A.; Kergall, F.; Da Silva, M.; Behar, F. *Org. Geochem.* **2008**, *39*, 1235–1242.
- (76) Li, M.; Cheng, D.; Pan, X.; Dou, L.; Hou, D.; Shi, Q.; Wen, Z.; Tang, Y.; Achal, S.; Milovic, M.; Tremblay, L. *Org. Geochem.* **2010**, *41*, 959–965.
- (77) Potz, S.; Wilkes, H.; Witt, M.; Horsfield, B. *Rapid Commun. Mass Spectrom.* **2010**, *24*, 1185–1197.
- (78) Qian, K.; Edwards, K. E.; Dechert, G. J.; Jaffe, S. B.; Green, L. A.; Olmstead, W. N. *Anal. Chem.* **2008**, *80*, 849–855.
- (79) Smith, D. F.; Schaub, T. M.; Kim, S.; Rodgers, R. P.; Rahimi, P.; Teclamariam, A.; Marshall, A. G. *Energy Fuels* **2008**, *22*, 2372–2378.
- (80) Grewer, D. M.; Young, R. F.; Whittal, R. M.; Fedorak, P. M. *Sci. Total Environ.* **2010**, *408*, 5997–6010.
- (81) Barrow, M. P.; Witt, M.; Headley, J. V.; Peru, K. M. *Anal. Chem.* **2010**, *82*, 3727–3735.
- (82) Sundman, O.; Simon, S.; Nordgard, E. L.; Sjoebloem, J. *Energy Fuels* **2010**, *24*, 6054–6060.
- (83) Shepherd, A. G.; Sorbie, K. S.; Thomson, G. B.; Westacott, R. E. *Energy Fuels* **2010**, *24*, 4387–4395.
- (84) Shepherd, A. G.; van Mispelaar, V.; Nowlin, J.; Genuit, W.; Grutters, M. *Energy Fuels* **2010**, *24*, 2300–2311.
- (85) Smith, B. E.; Sutton, P. A.; Lewis, A. C.; Dunsmore, B.; Fowler, G.; Krane, J.; Lutnaes, B. F.; Brandal, O.; Sjoblom, J.; Rowland, S. J. *J. Sep. Sci.* **2007**, *30*, 375–380.
- (86) Sutton, P. A.; Smith, B. E.; Rowland, S. J. *Rapid Commun. Mass Spectrom.* **2010**, *24*, 3195–3204.
- (87) Mapolelo, M. M.; Rodgers, R. P.; Blakney, G. T.; Yen, A. T.; Asomaning, S.; Marshall, A. G. *Int. J. Mass Spectrom.* **2011**, *300*, 149–157.
- (88) Mapolelo, M. M.; Stanford, L. A.; Rodgers, R. P.; Yen, A. T.; Debord, J. D.; Asomaning, S.; Marshall, A. G. *Energy Fuels* **2009**, *23*, 349–355.
- (89) Czarnecki, J. *Energy Fuels* **2009**, *23*, 1253–1257.
- (90) Stanford, L. A.; Rodgers, R. P.; Marshall, A. G.; Czarnecki, J.; Wu, X. A.; Taylor, S. *Energy Fuels* **2007**, *21*, 973–981.
- (91) Freitas, L. S.; Von Muehlen, C.; Bortoluzzi, J. H.; Zini, C. A.; Fortuny, M.; Dariva, C.; Coutinho, R. C. C.; Santos, A. F.; Caramao, E. B. *J. Chromatogr., A* **2009**, *1216*, 2860–2865.
- (92) Muller, H.; Pauchard, V. O.; Hajji, A. A. *Energy Fuels* **2009**, *23*, 1280–1288.
- (93) Zhang, Y.; Xu, C.; Shi, Q.; Zhao, S.; Chung, K. H.; Hou, D. *Energy Fuels* **2010**, *24*, 6321–6326.
- (94) Shi, Q.; Zhao, S.; Xu, Z.; Chung, K. H.; Zhang, Y.; Xu, C. *Energy Fuels* **2010**, *24*, 4005–4011.
- (95) Shi, Q.; Hou, D.; Chung, K. H.; Xu, C.; Zhao, S.; Zhang, Y. *Energy Fuels* **2010**, *24*, 2545–2553.
- (96) Mullins, O. C.; Martinez-Haya, B.; Marshall, A. G. *Energy Fuels* **2008**, *22*, 1765–1773.
- (97) Pinkston, D. S.; Duan, P.; Gallardo, V. A.; Habicht, S. C.; Tan, X.; Qian, K.; Gray, M. R.; Mullen, K.; Kenttamaa, H. I. *Energy Fuels* **2009**, *23*, 5564–5570.
- (98) Juyal, P.; Yen, A. T.; Rodgers, R. P.; Allenson, S. J.; Wang, J.; Creek, J. *Energy Fuels* **2010**, *24*, 2320–2326.
- (99) Smith, D. F.; Klein, G. C.; Yen, A. T.; Squicciarini, M. P.; Rodgers, R. P.; Marshall, A. G. *Energy Fuels* **2008**, *22*, 3112–3117.
- (100) Purcell, J. M.; Merdrignac, I.; Rodgers, R. P.; Marshall, A. G.; Gauthier, T.; Guibard, I. *Energy Fuels* **2010**, *24*, 2257–2265.
- (101) Mullins, O. C.; Ventura, G. T.; Nelson, R. K.; Betancourt, S. S.; Raghuraman, B.; Reddy, C. M. *Energy Fuels* **2008**, *22*, 496–503.
- (102) Mullins, O. C.; Rodgers, R. P.; Weinheber, P. K.; Klein, G. C.; Venkataramanan, L.; Andrews, A. B.; Marshall, A. G. *Energy Fuels* **2006**, *20*, 2488–2456.
- (103) Betancourt, S. S.; Ventura, G. T.; Pomerantz, A. E.; Viloria, O.; Dubost, F. X.; Zuo, J.; Monson, G.; Bustamante, D.; Purcell, J. M.; Nelson, R. K.; Rodgers, R. P.; Reddy, C. M.; Marshall, A. G.; Mullins, O. C. *Energy Fuels* **2009**, *23*, 1178–1188.
- (104) Pomerantz, A. E.; Ventura, G. T.; McKenna, A. M.; Canas, J. A.; Auman, J.; Koerner, K.; Curry, D.; Nelson, R. K.; Reddy, C. M.; Rodgers, R. P.; Marshall, A. G.; Peters, K. E.; Mullins, O. C. *Org. Geochem.* **2010**, *41*, 812–821.
- (105) Tran, T. C.; Logan, G. A.; Grossjean, E.; Ryan, D.; Marriott, P. J. *Geochim. Cosmochim. Acta* **2010**, *74*, 6468–6484.
- (106) Wei, Z.; Mankiewicz, P.; Walters, C. C.; Qian, K.; Phan, N. T.; Madincea, M. E.; Nguyen, P. T. *Org. Geochem.* **2011**, *42*, 121–133.
- (107) Springer, M. V.; Garcia, D. F.; Goncalves, F. T.; Landau, L.; Azevedo, D. A. *Org. Geochem.* **2010**, *41*, 1013–1018.
- (108) Sharipova, N. S.; Budnikov, G. K.; Uspenskii, B. V.; Kayukova, G. P. *J. Anal. Chem.* **2010**, *65*, 438–444.
- (109) Aguiar, A.; Aguiar, H. G. M.; Azevedo, D. A.; Aquino Neta, F. R. *Energy Fuels* **2011**, *25*, 1060–1065.
- (110) Avila, B. M.; Aguiar, A.; Gomes, A. O.; Azevedo, D. A. *Org. Geochem.* **2010**, *41*, 863–866.
- (111) Cortes, J. E.; Rincon, J. M.; Jaramillo, J. M.; Philip, R. P.; Allen, J. S. *Amer. Earth Sciences* **2010**, *29*, 198–231.
- (112) Juyal, P.; McKenna, A. M.; Yen, A. T.; Rodgers, R. P.; Reddy, C. M.; Nelson, R. K.; Andrews, A. B.; Atolia, E.; Allenson, S. J.; Mullins, O. C.; Marshall, A. G. *Energy Fuels* **2011**, *25*, 172–182.
- (113) Simoneit, B. R. T.; Deamer, D. W.; Kompanichenko, V. *Appl. Geochem.* **2009**, *24*, 303–309.
- (114) Sarmah, M. K.; Borthakur, A.; Dutta, A. *Bull. Mater. Sci.* **2010**, *33*, 509–515.
- (115) Sarmah, M. K.; Borthakur, A.; Dutta, A. *Petr. Sci. Technol.* **2010**, *28*, 1068–1077.
- (116) Barman, B. N.; Cebolla, V. L.; Membrado, L. *Crit. Rev. Anal. Chem.* **2000**, *30*, 75–120.
- (117) Coto, B.; Martos, C.; Pena, J. L.; Espada, J. J.; Robustillo, M. D. *Fuel* **2008**, *87*, 2090–2094.
- (118) Coto, B.; Martos, C.; Espada, J. J.; Robustillo, M. D.; Pena, J. L. *Fuel* **2010**, *89*, 1087–1094.
- (119) Coto, B.; Coutinho, J. A.; Martos, C.; Robustillo, M. D.; Espada, J. J.; Pena, J. L. *Energy Fuels* **2011**, *25*, 1153–1160.
- (120) Espada, J. J.; Coutinho, J. A.; Pena, J. L. *Energy Fuels* **2010**, *24*, 1837–1843.
- (121) Coto, B.; Martos, C.; Espada, J. J.; Robustillo, M. D.; Merino-Garcia, D.; Pena, J. L. *Energy Fuels* **2011**, *25*, 487–492.
- (122) Martos, C.; Coto, B.; Espada, J. J.; Robustillo, M. D.; Pena, J. L.; Merino-Garcia, D. *Energy Fuels* **2010**, *24*, 2221–2226.
- (123) Coto, B.; Martos, C.; Espada, J. J.; Robustillo, M. D.; Merino-Garcia, D.; Pena, J. L. *Energy Fuels* **2011**, *25*, 1707–1713.
- (124) Bauserman, J. W.; Mushrush, G. W.; Willauer, H.; Wynne, J. H.; Phillips, J. P.; Buckley, J. L.; Williams, F. W. *Petr. Sci. Technol.* **2010**, *28*, 1761–1769.
- (125) Wang, F. C.; Walters, C. C. *Anal. Chem.* **2007**, *79*, 5642–5650.
- (126) Bruno, T. J. *Ind. Eng. Chem. Res.* **2006**, *45*, 4371–4380.
- (127) Bruno, T. J.; Ott, L. S.; Lovestead, T. M.; Huber, M. L. *J. Chromatogr., A* **2010**, *1217*, 2708.
- (128) Ott, L. S.; Bruno, T. J. *Energy Fuels* **2008**, *22*, 2861–2868.
- (129) Bruno, T. J.; Smith, B. L. *Energy Fuels* **2006**, *20*, 2109–2116.
- (130) Bachler, C.; Schober, S.; Mittelbach, M. *Energy Fuels* **2010**, *24*, 2086–2090.
- (131) Boczkaj, G.; Przyjazny, A.; Kamiński, M. *Anal. Bioanal. Chem.* **2011**, *399*, 3253–3260.
- (132) Satyro, M. A.; Yarranton, H. *Energy Fuels* **2009**, *23*, 3960–3970.
- (133) Wang, Y.; Chen, Q.; Norwood, D. L.; McCaffrey, J. J. *Liq. Chromatogr. Relat. Technol.* **2010**, *33*, 1082–1115.
- (134) Maikhunthod, B.; Morrison, P. D.; Small, D. M.; Marriott, P. J. *J. Chromatogr., A* **2010**, *1217*, 1522–1529.
- (135) Eyes, G. T.; Urban, S.; Morrison, P. D.; Marriott, P. J. *J. Chromatogr., A* **2008**, *1214*, 134–142.
- (136) Frysinger, G. S.; Gaines, R. B.; Xu, L.; Reddy, C. M. *Environ. Sci. Technol.* **2003**, *37*, 1653–1662.
- (137) Frysinger, G. S.; Gaines, R. B.; Reddy, C. M. *Environ. Forensics* **2002**, *3*, 27–34.
- (138) Lemkau, K. L.; Peacock, E. E.; Nelson, R. K.; Ventura, G. T.; Kovacs, J. L.; Reddy, C. M. *Mar. Pollut. Bull.* **2010**, *60*, 2123–2129.

- (139) Peacock, E. A.; Hampson, G. R.; Nelson, R. K.; Xu, L.; Frysinger, G. S.; Gaines, R. B.; Farrington, J. W.; Tripp, B. W.; Reddy, C. M. *Mar. Pollut. Bull.* **2007**, *54*, 214–225.
- (140) Arey, S. J.; Nelson, R. K.; Reddy, C. M. *Environ. Sci. Technol.* **2007**, *41*, 5738–5746.
- (141) Arey, S. J.; Nelson, R. K.; Plata, D. L.; Reddy, C. M. *Environ. Sci. Technol.* **2007**, *41*, 5747–5755.
- (142) Camili, R.; Bingham, B.; Reddy, C. M.; Nelson, R. K.; Duryea, A. N. *Mar. Pollut. Bull.* **2009**, *58*, 1505–1513.
- (143) Farwell, C.; Reddy, C. M.; Peacock, E. A.; Nelson, R. K.; Washburn, L.; Valentine, D. L. *Environ. Sci. Technol.* **2009**, *43*, 3542–3548.
- (144) Wang, F. C. *J. Chromatogr., A* **2008**, *1188*, 274–280.
- (145) Van Geem, K. M.; Pyl, S. P.; Reyniers, M.-F.; Vercammen, J.; Beens, J.; Marin, G. B. *J. Chromatogr., A* **2010**, *1217*, 6623–6633.
- (146) Dutriez, T.; Courtiade, M.; Thiebaut, D.; Dulot, H.; Bertocini, F.; Vial, J.; Hennion, M.-C. *J. Chromatogr., A* **2009**, *1216*, 2905–2912.
- (147) Dutriez, T.; Courtiade, M.; Thiebaut, D.; Dulot, H.; Hennion, M.-C. *Fuel* **2010**, *89*, 2338–2345.
- (148) Dutriez, T.; Courtiade, M.; Thiebaut, D.; Dulot, H.; Borras, J.; Bertocini, F.; Hennion, M.-C. *Energy Fuels* **2010**, *24*, 4430–4438.
- (149) Adam, F.; Bertocini, F.; Dartiguelongue, C.; Marchand, K.; Thiebaut, D.; Hennion, M.-C. *Fuel* **2009**, *88*, 938–946.
- (150) Zhang, Z. G.; Guo, S.; Zhao, S.; Yan, G.; Song, L.; Chen, C. *Energy Fuels* **2009**, *23*, 374–385.
- (151) Simon, S.; Nenninglsland, A. L.; Herschbach, E.; Sjoblom, J. *Energy Fuels* **2010**, *24*, 1043–1050.
- (152) Nenninglsland, A. L.; Simon, S.; Sjoblom, J. *Energy Fuels* **2010**, *24*, 6501–6505.
- (153) Boduszyński, M. M. *Energy Fuels* **1987**, *1*, 2–11.
- (154) Altgelt, K. H. *J. Appl. Polym. Sci.* **1965**, *9*, 3389–3393.
- (155) Behrouzi, M.; Luckman, P. F. *Energy Fuels* **2008**, *22*, 1792–1798.
- (156) Trejo, F.; Ancheyta, J. *Ind. Eng. Chem.* **2007**, *46*, 7571–7579.
- (157) Kharrat, A. M. *Energy Fuels* **2009**, *23*, 828–834.
- (158) Kok, W. T.; Tudos, A. J.; Grutters, M.; Shepherd, A. G. *Energy Fuels* **2011**, *25*, 208–214.
- (159) Nolte, T.; Andersson, J. T. *Anal. Bioanal. Chem.* **2009**, *395*, 1843–1852.
- (160) Robbins, W. K. *J. Chromatogr. Sci.* **1998**, *36*, 457–466.
- (161) Kaminski, M.; Kartanowicz, R.; Gilgenast, E.; Namiesnik, J. *Crit. Rev. Anal. Chem.* **2005**, *35*, 193–216.
- (162) Oro, N. E.; Lucy, C. A. *J. Chromatogr., A* **2010**, *1217*.
- (163) Tomic, T.; Babic, S.; Nasipak, N. U.; Ruszkowski, M. F.; Skrobonja, L.; Kastelan-Macan, M. *J. Chromatogr., A* **2009**, *1216*, 3819–3824.
- (164) Borgund, A. E.; Erstad, K.; Barth, T. *J. Chromatogr., A* **2007**, *1149*, 189–196.
- (165) Borgund, A. E.; Erstad, K.; Barth, T. *Energy Fuels* **2007**, *21*, 2816–2826.
- (166) Mao, D.; Van De Weghe, H.; Diels, L.; De Brucker, N.; Lookman, R.; Vanerman, G. *J. Chromatogr., A* **2008**, *1179*, 33–40.
- (167) Kharrat, A. M.; Zacharia, J.; Cherian, V. J.; Anyatonwu, A. *Energy Fuels* **2007**, *21*, 3618–3621.
- (168) Boduszyński, M. M.; McKay, J. F.; Lathan, D. R. *Asphalt Pav. Techn.* **1980**, *49*, 123–143.
- (169) Schabron, J. F.; Rovani, J. F., Jr.; Sanderson, M. M. *Energy Fuels* **2010**, *24*, 5984–5996.
- (170) Zuo, J. Y.; Mullins, O. C.; Freed, D. E.; Zhang, D. *J. Chem. Eng. Data* **2010**, *55*, 2964–2969.
- (171) Acevedo, A.; Castro, A.; Vasquez, E.; Marcan, F.; Ranaudo, M. A. *Energy Fuels* **2010**, *24*, 5921–5933.
- (172) Solum, M. S.; Pugmire, R. J.; Grant, D. M. *Energy Fuels* **1989**, *3*, 187–193.
- (173) Storm, D. A.; Edwards, J. C.; DeCanio, S. J.; Sheau, E. Y. *Energy Fuels* **1994**, *8*, 561–566.
- (174) Kelemen, S. R.; Afeworki, M.; Gorbatty, M. L.; Sansone, M.; Kwiatek, P. J.; Walters, C. C.; Freund, H.; Siskin, M.; Bence, A. E.; Curry, D. J.; Solum, M.; Pugmire, R. J.; Vandebroucke, M.; Leblond, M.; Behar, F. *Energy Fuels* **2007**, *21*, 1548–1561.
- (175) Kelemen, S. R.; Walters, C. C.; Kwiatek, P. J.; Freund, H.; Afeworki, M.; Sansone, M.; Lamberti, W. A.; Pottorf, R. J.; Machel, H. G.; Peters, K. E.; Bolin, T. *Geochim. Cosmochim. Acta* **2010**, *74*, 5305–5332.
- (176) Yang, Z.; Hirasaki, G. J. *J. Magn. Reson.* **2008**, *192*, 280–293.
- (177) Martos, C.; Coto, B.; Espada, J. J.; Robustillo, M. D.; Gomez, S.; Pena, J. L. *Energy Fuels* **2008**, *22*, 708–714.
- (178) Zielinski, L.; Saha, I.; Freed, D. E.; Hurlimann, M. D. *Langmuir* **2010**, *26*, 5014–5021.
- (179) Liszta, N. V.; Freed, D. E.; Sen, P.; Song, Y.-Q. *Energy Fuels* **2009**, *23*, 1189–1193.
- (180) Durand, E.; Clemancey, M.; Quoineaud, A.-A.; Verstraete, J.; Espinat, D.; Lancelin, J.-M. *Energy Fuels* **2008**, *22*, 2604–2610.
- (181) Kawashima, H.; Takanohashi, T.; Iino, M.; Matsukawa, S. *Energy Fuels* **2008**, *22*, 3989–3993.
- (182) Mutina, A. R.; Hurlimann, M. D. *J. Phys. Chem. A* **2008**, *112*, 3291–3301.
- (183) Callema, V.; Iwanski, P.; Nali, M.; Scotti, R.; Montanari, L. *Energy Fuels* **1995**, *9*, 225–230.
- (184) Murphy, P. D.; Gerstein, B. C.; Weinberg, V. L.; Yen, T. F. *Anal. Chem.* **1982**, *54*, 522–525.
- (185) Durand, E.; Clemancey, M.; Lancelin, J.-M.; Verstraete, J.; Espinat, D.; Quoineaud, A.-A. *Energy Fuels* **2010**, *24*, 1051–1062.
- (186) Bouhadda, Y.; Florian, P.; Bendedouch, D.; Fergoug, T.; Bormann, D. *Fuel* **2010**, *89*, 522–526.
- (187) Ryder, A. G. Analysis of Crude Petroleum Oils Using Fluorescence Spectroscopy. In *Reviews in Fluorescence 2005*; Springer-Science + Business Media, Inc.: New York, 2005; Vol. 2, pp 169–198.
- (188) Blamey, N. J. F.; Ryder, A. G. *Rev. Fluorescence* **2007**, *4*, 299–334.
- (189) Blamey, N. J. F.; Conliffe, J.; Parnell, J.; Ryder, A. G.; Feely, M. *Geofluids* **2009**, *9*, 330–337.
- (190) Andrews, A. B.; Schneider, M. H.; Canas, J.; Freitas, E.; Song, Y.-Q.; Mullins, O. C. *J. Dispersion Sci. Technol.* **2008**, *29*, 171–183.
- (191) Ruiz-Morales, Y.; Mullins, O. C. *Energy Fuels* **2009**, *23*, 1169–1177.
- (192) Klee, T.; Masterson, T.; Miller, B.; Barrasso, E.; Bell, J.; Lepkowicz, R.; West, J.; Haley, J. E.; Schmitt, D. L.; Flikkema, J. L.; Cooper, T. M.; Ruiz-Morales, Y.; Mullins, O. C. *Energy Fuels* **2011**, DOI: 10.1021/ef101549k.
- (193) Orbulescu, J.; Mullins, O. C.; Leblanc, R. M. *Langmuir* **2010**, *26*.
- (194) Orbulescu, J.; Mullins, O. C.; Leblanc, R. M. *Langmuir* **2010**, *26*, 15265–15271.
- (195) Andrews, A. B.; Guerra, R. E.; Mullins, O. C.; Sen, P. N. *J. Phys. Chem. A* **2006**, *110*, 8093–8097.
- (196) Schneider, M. H.; Andrews, A. B.; Mitra-Kirtley, S.; Mullins, O. C. *Energy Fuels* **2007**, *21*, 2875–2882.
- (197) Groenzin, H.; Mullins, O. C. *J. Phys. Chem. A* **1999**, *103*, 11237–11245.
- (198) Strausz, O. P.; Safarik, I.; Lown, E. M.; Morales-Izquierdo, A. *Energy Fuels* **2008**, *22*, 1156–1166.
- (199) Mullins, O. C. *Energy Fuels* **2010**, *24*, 2179–2207.
- (200) Souza, R.; Nicodem, D. E.; Garden, S. J.; Correa, R. J. *Energy Fuels* **2010**, *24*, 1135–1138.
- (201) Hasan, M. A.; Fulem, M.; Bazyleva, A.; Shaw, J. M. *Energy Fuels* **2009**, *23*, 5012–5021.
- (202) Zhao, B.; Becerra, M.; Shaw, J. M. *Energy Fuels* **2009**, *23*, 4431–4437.
- (203) Indo, K.; Ratulowski, J.; Dindoruk, B.; Gao, J.; Zuo, J.; Mullins, O. C. *Energy Fuels* **2009**, *23*, 4460–4469.
- (204) Mostowfi, F.; Indo, K.; Mullins, O. C.; McFarlane, R. *Energy Fuels* **2009**, *23*, 1194–1200.
- (205) Ching, T. M.; Pomerantz, M.-J.; Andrews, A. E.; Dryden, A. B.; Schroeder, P.; Mullins, R.; Harrison, O. C. *Energy Fuels* **2010**, *24*, 5028–5037.

- (206) Sirota, E. B. *Energy Fuels* **2005**, *19*, 1290–1296.
- (207) Andreatta, G.; Bostrom, N.; Mullins, O. C. *Langmuir* **2005**, *21*, 2728–2736.
- (208) Xing, C.; Hilts, R. W.; Shaw, J. M. *Energy Fuels* **2010**, *24*.
- (209) Oye, G.; Silset, A.; Knag, M.; Orevoll, B.; Sjøblom, J. J. *Dispersion Sci. Technol.* **2005**, *26*, 665–671.
- (210) Sheu, E. Y. *J. Phys.: Condens. Matter* **2006**, *18*, S2485–S2498.
- (211) Barre, L.; Sal, S.; Palermo, T. *Langmuir* **2008**, *24*, 3709–3717.
- (212) Gawrys, K. L.; Blankenship, G. A.; Kilpatrick, P. K. *Langmuir* **2006**, *22*, 4487–4497.
- (213) Verruto, V. J.; Kilpatrick, P. K. *Energy Fuels* **2007**, *21*, 1217–1225.
- (214) Headen, T. F.; Boek, E. S.; Stellbrink, J.; Scheven, U. M. *Langmuir* **2009**, *25*, 422–428.
- (215) Alvarez, G.; Jestin, J.; Argillier, J. F.; Langevin, D. *Langmuir* **2009**, *25*, 3985–3990.
- (216) Verruto, V. J.; Kilpatrick, P. K. *Langmuir* **2008**, *24*, 12807–12822.
- (217) Ridi, F.; Verdial, N.; Baglioni, P.; Sheu, E. Y. *Fuel* **2008**, *88*, 319–325.
- (218) Zeng, H.; Song, Y.-Q.; Johnson, D. L.; Mullins, O. C. *Energy Fuels* **2009**, *23*, 1201–1208.
- (219) Sedghi, M.; Goual, L. *Energy Fuels* **2010**, *24*, 2275–2280.
- (220) Rogel, E. *Energy Fuels* **2008**, *22*, 3922–3929.
- (221) Bagheri, S. R.; Bazyleva, A.; Gray, M. R.; McCaffrey, W. C.; Shaw, J. M. *Energy Fuels* **2010**, *24*, 4327–4332.
- (222) Klein, M. T.; Virk, P. S. *Energy Fuels* **2008**, *22*, 2175–2182.
- (223) Wei, W.; Bennett, C. A.; Tanaka, R.; Hou, G.; Klein, M. T. *Fuel Process. Technol.* **2008**, *89*, 344–349.
- (224) Campbell, D. M.; Bennett, C. A.; Hou, Z.; Klein, M. T. *Ind. Eng. Chem. Res.* **2009**, *48*, 1683–1693.
- (225) Ventura, G. T.; Raghuraman, B.; Nelson, R. K.; Mullins, O. C.; Reddy, C. M. *Org. Geochem.* **2010**, *41*, 1026–1035.
- (226) Ventura, G. T.; Hall, G. J.; Nelson, R. K.; Frysinger, G. S.; Raghuraman, B.; Pomerantz, A. E.; Mullins, O. C.; Reddy, C. M. *J. Chromatogr., A* **2011**, *1218*, 2584–2592.
- (227) Nouvelle, X.; Coutrot, D. *Org. Geochem.* **2010**, *41*, 981–985.
- (228) Fernandez-Varela, R.; Andrade, J. M.; Muniategui, S.; Prada, D. *J. Chromatogr., A* **2010**, *1217*, 8279–8289.
- (229) Chen, J.; Mclean, N.; Hager, D. *Energy Fuels* **2011**, *25*.
- (230) Ha, H. Z.; Ring, Z.; Liu, S. *Petr. Sci. Technol.* **2008**, *26*, 7–28.
- (231) Hu, M.; Yeo, I.; Park, E.; Kim, Y. H.; Yoo, J.; Kim, E.; No, M.; Koh, J.; Kim, S. *Anal. Chem.* **2010**, *82*, 211–218.
- (232) Ahmed, A.; Cho, Y. J.; No, M.; Koh, J.; Tomczyk, N.; Giles, K.; Yoo, J. S.; Kim, S. *Anal. Chem.* **2011**, *83*, 77–83.